

PCR-Based Molecular Diagnosis (Literature Review)

Chaoran Jing

11-13-2013

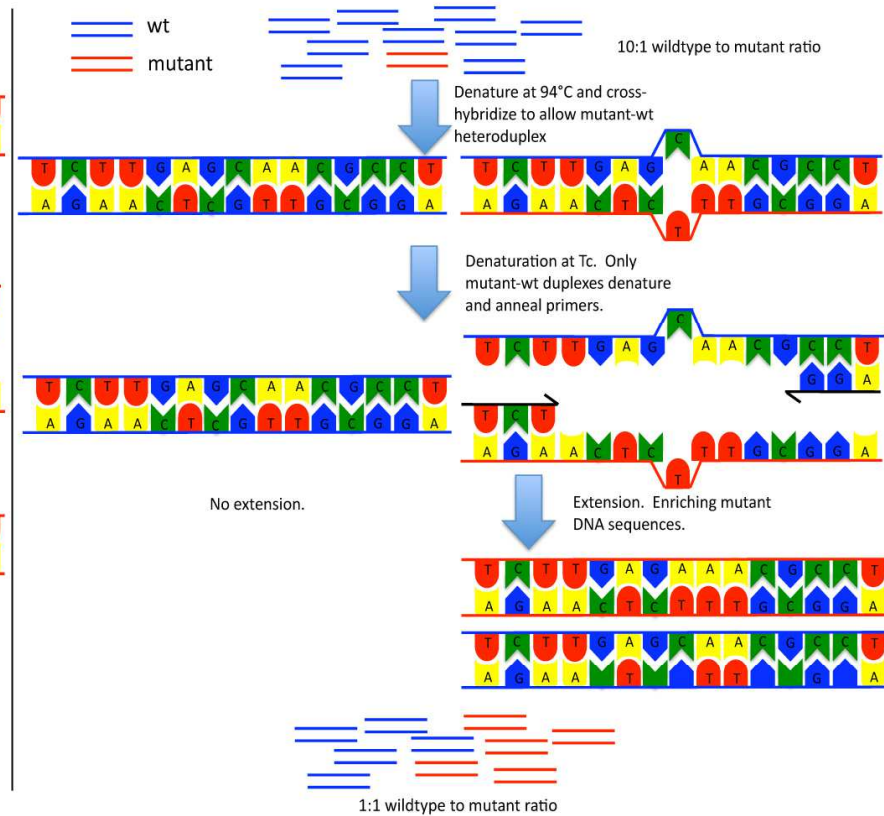
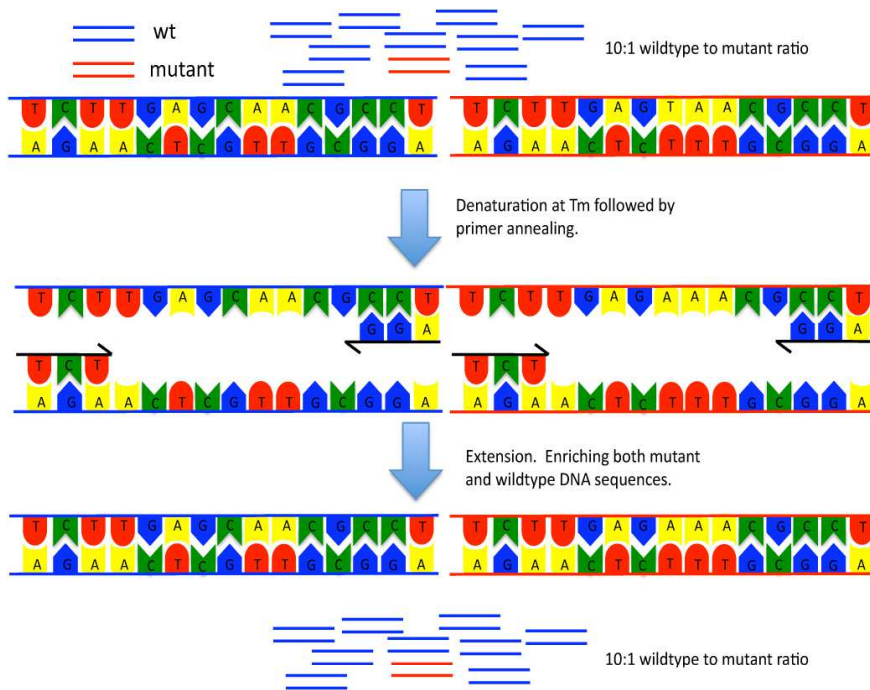
Outline

- Background: cancer biomarker in blood plasma
- COLD-PCR
 - How it works
 - Different protocols
 - Detection technologies
 - Clinical applications
- Digital PCR
 - How it works
 - Comparison with qPCR
 - Instrumentation
 - Clinical applications
- COLD-PCR and digital PCR
- Detection of tri- and hexa-nucleotide repeat expansion

Cancer biomarkers in blood plasma

- Cancer cells release short DNA fragments (150 ~ 250 bp) into circulation system: cfDNA.
- Some mutations (TP53; KRAS etc) are tumor specific and thus can be used as biomarkers.
- Detecting these mutants in blood plasma is useful for cancer diagnosis and prognosis.
- Challenge is: there is also overwhelming amount of wt DNA in plasma.
- Solutions:
 - Enrich mutant DNA -> COLD-PCR
 - Use highly sensitive detection methods -> Digital PCR

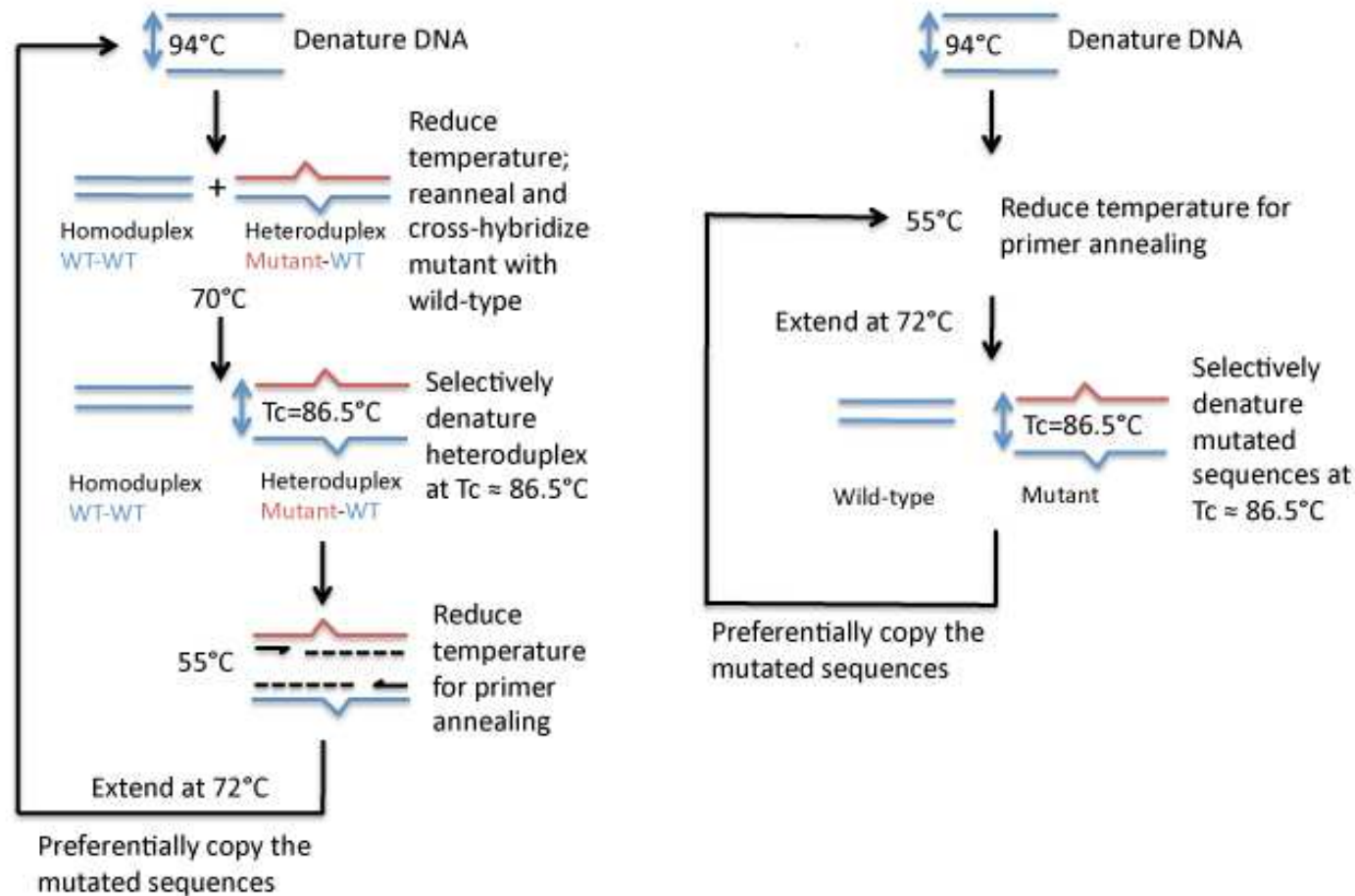
COLD-PCR: how it works



Conventional PCR

COLD-PCR

COLD-PCR: various protocols



Full COLD-PCR
For enrichment of all mutations

Fast COLD-PCR
For enrichment of T_m -reducing mutations

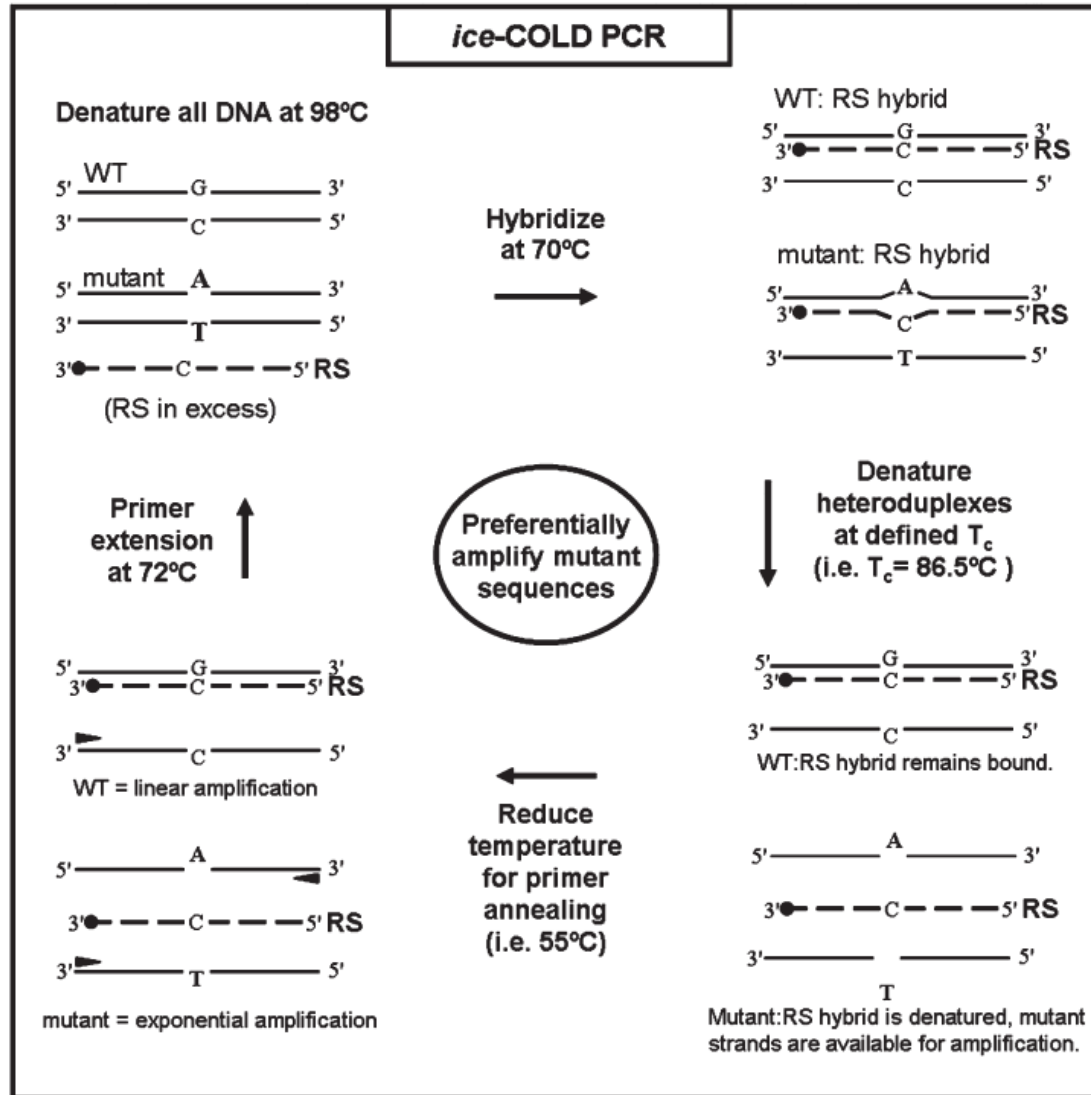
COLD-PCR: full Vs. fast

Table 1 Mutation prevalence for various types of somatic mutations in human cancer and mutation enrichment anticipated via COLD-PCR

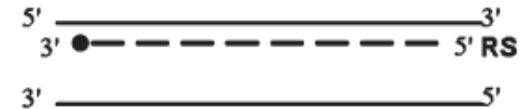
Mutation	Prevalence of somatic mutation in cancer ²⁷					COLD-PCR	COLD-PCR
	Lung (%)	Colon (%)	Breast (%)	Melanoma (%)	Glioma (%)	Enrichment (full COLD-PCR) ^e , all mutations	Enrichment (fast COLD-PCR) ^e , T_m -decreasing mutations
C:G → T:A ^a	37	78	37	92	97	5–12-fold	10–100-fold
C:G → A:T ^a	29	6	15	2	1		
T:A → A:T ^b	4	2	1	2	0	5–8-fold	None
C:G → G:C ^b	15	4	36	1	0		
T:A → G:C ^c	3	2	4	~0	0	3–5-fold	None
T:A → C:G ^c	6	8	3	2	0		
Microdeletions and insertions ^d	6	~0	3	1	2	>50-fold one or more rounds	>100-fold

^aThese mutations generally reduce the T_m of a DNA sequence. ^bThese mutations generally retain the T_m of a DNA sequence. ^cThese mutations generally increase the T_m of a DNA sequence. ^dThese mutations may increase, retain or decrease the T_m of a DNA sequence. ^eThe enrichment is defined as the fold-increase of the prevalence of a mutation relative to performing regular PCR.

Ice-COLD-PCR



Reference Sequence (RS)

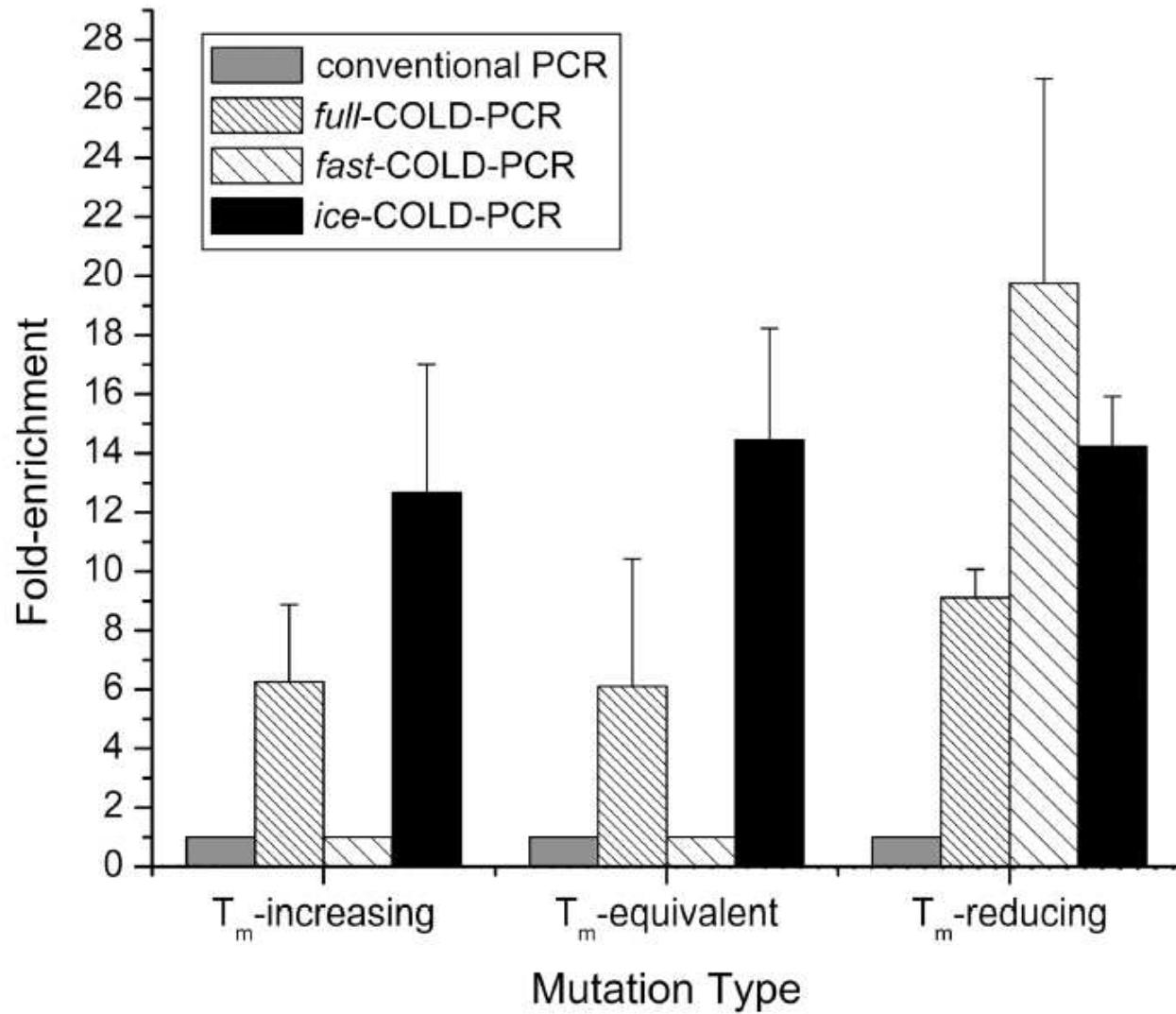


e.g. RS = 60 nt and RS = 90 nt used in this work

RS sequence properties:

- Complementary to WT sense-strand sequence
- 3'-PO₄ prevents polymerase extension
- ≤5 bp overlap with amplicon primers to prevent primer binding
- Selectively enhances denaturation of mutated sequences at the critical denaturation temperature (T_c)

Ice-COLD-PCR



COLD-PCR: T_c

- **Definition:** for each DNA sequence, there is a critical denaturation temperature (T_c) that is lower than T_m and below which PCR efficiency decreases abruptly.

- **Experimentally:** For example, a 167 bp p53 sequence used in the present study amplifies well when PCR denaturation temperature is set to 87°C, amplifies modestly at 86.5°C and yields no detectable product when PCR denaturation is set to 86°C or below. Therefore, in this example, $T_c \approx 86.5^\circ\text{C}$.

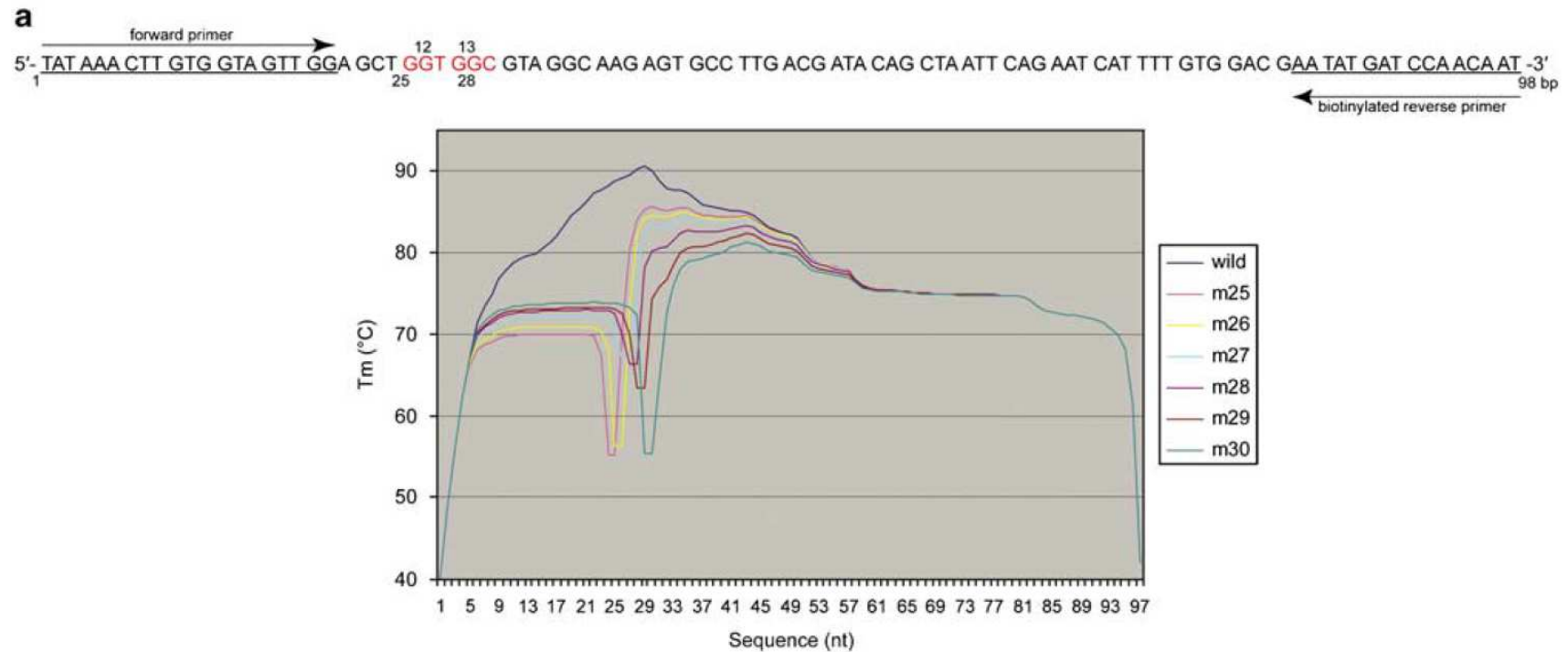
J. Li, et al. G.M. Makrigiorgos, Nat. Medicine 2008, 14, 579

- **Empirically:** The T_c is typically 1 °C below the experimentally derived amplicon T_m . Defining the T_c in this man-

C.A. Milbury, et al, G.M. Makrigiorgos, Clin. Chem. 2009, 55, 2031

COLD-PCR: Computation

- Computation methods like MeltSim and Poland Algorithm can help to generate melting profile.

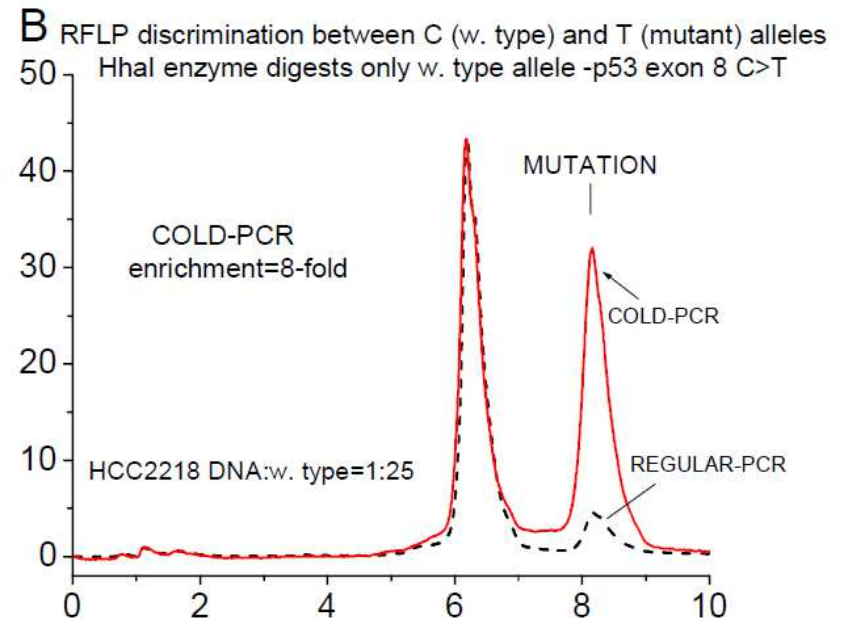
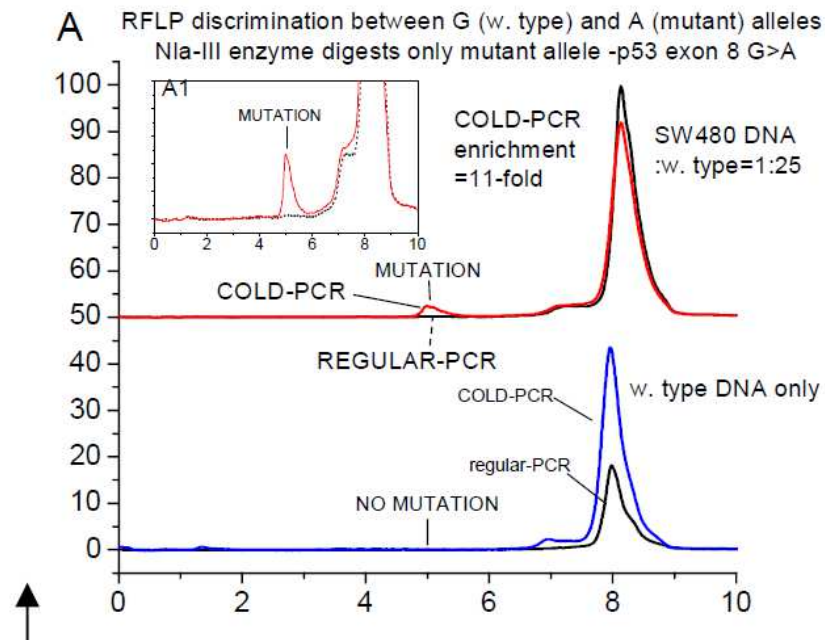


COLD-PCR: detection

- COLD-PCR is an enrichment technique. We need to pair it with another assay for detection.
- Restriction fragment length polymorphism (RFLP).
 - Offline detection by gel or HPLC.
 - COLD-PCR can improve detection limit by 10~20 fold (HPLC), which means 5% -> 65%.
- DNA sequencing and MS.
 - Not available in lab.
- COLD-PCR with Taqman
 - Online detection with the PCR machine
 - Can detect ~ 0.8% mutant among wt DNA.
- High resolution melting analysis (HRMA).
 - Online detection with PCR machine
- Digital PCR. (Will discuss later)

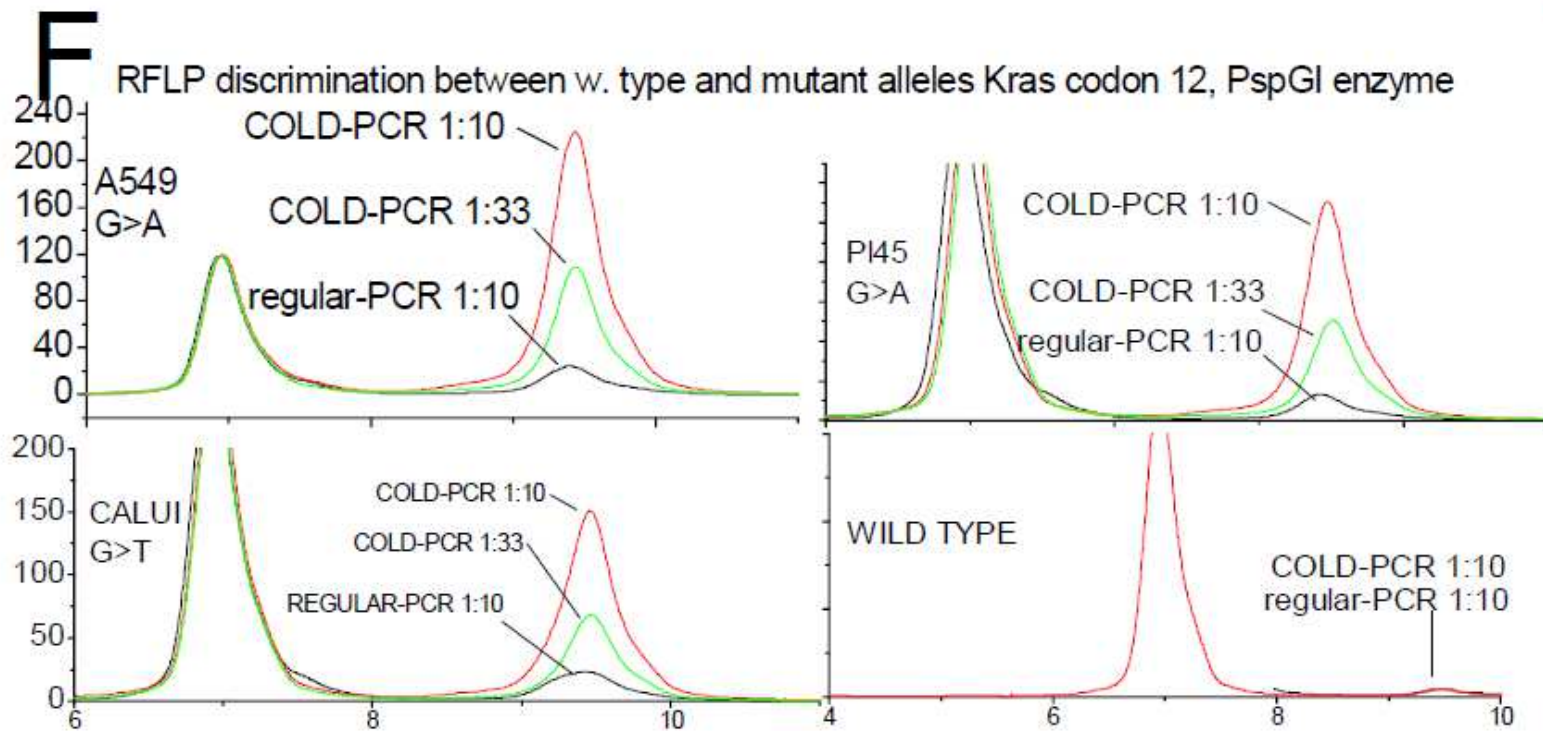
COLD-PCR with RFLP

full-COLD-PCR

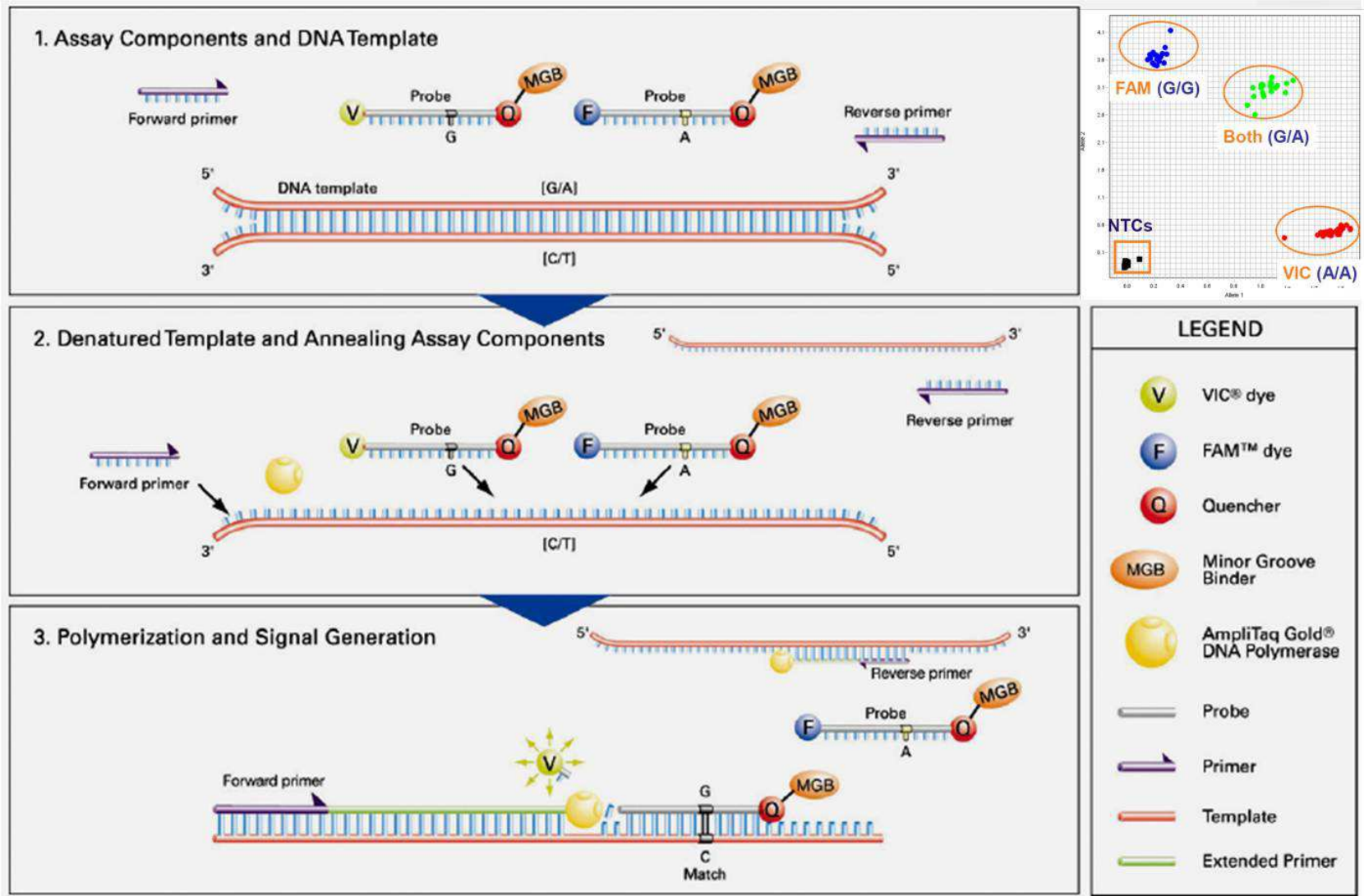


COLD-PCR with RFLP

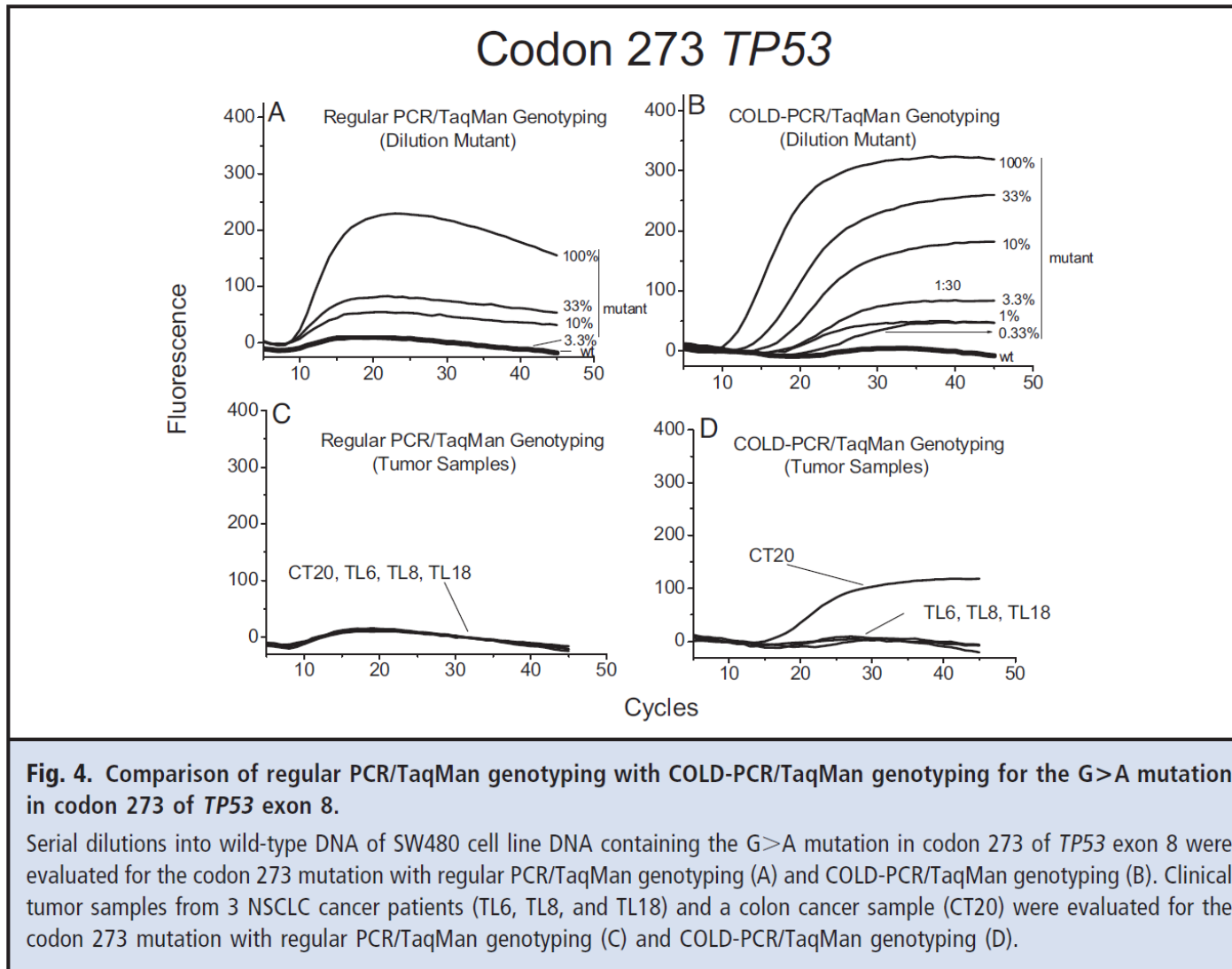
fast –COLD-PCR



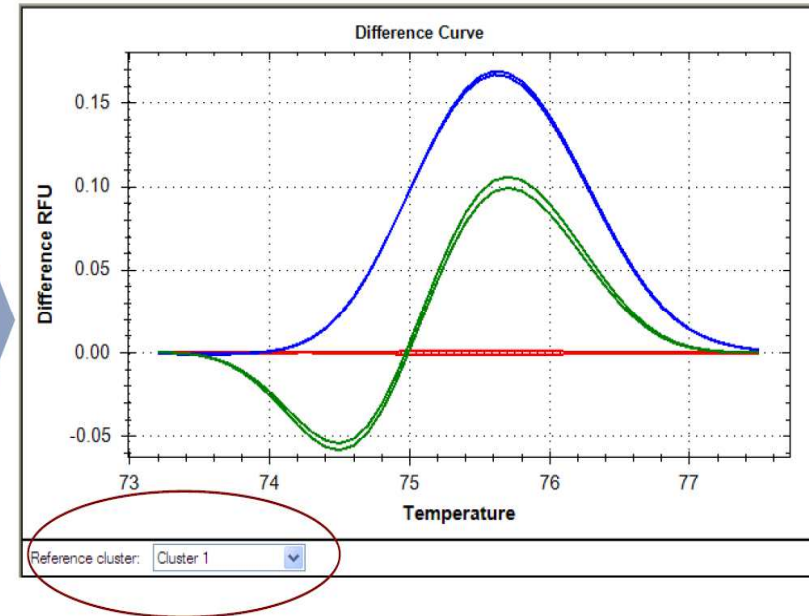
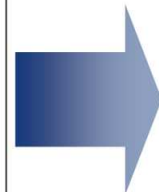
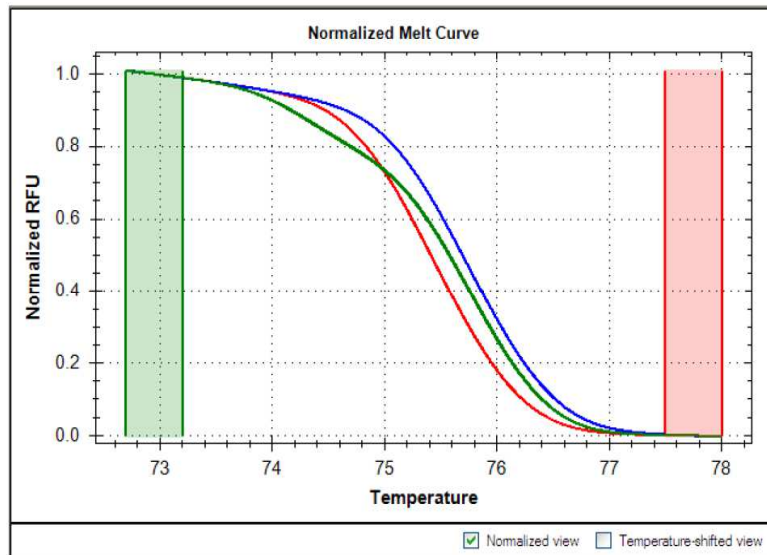
Taqman qPCR technology



COLD-PCR with Taqman

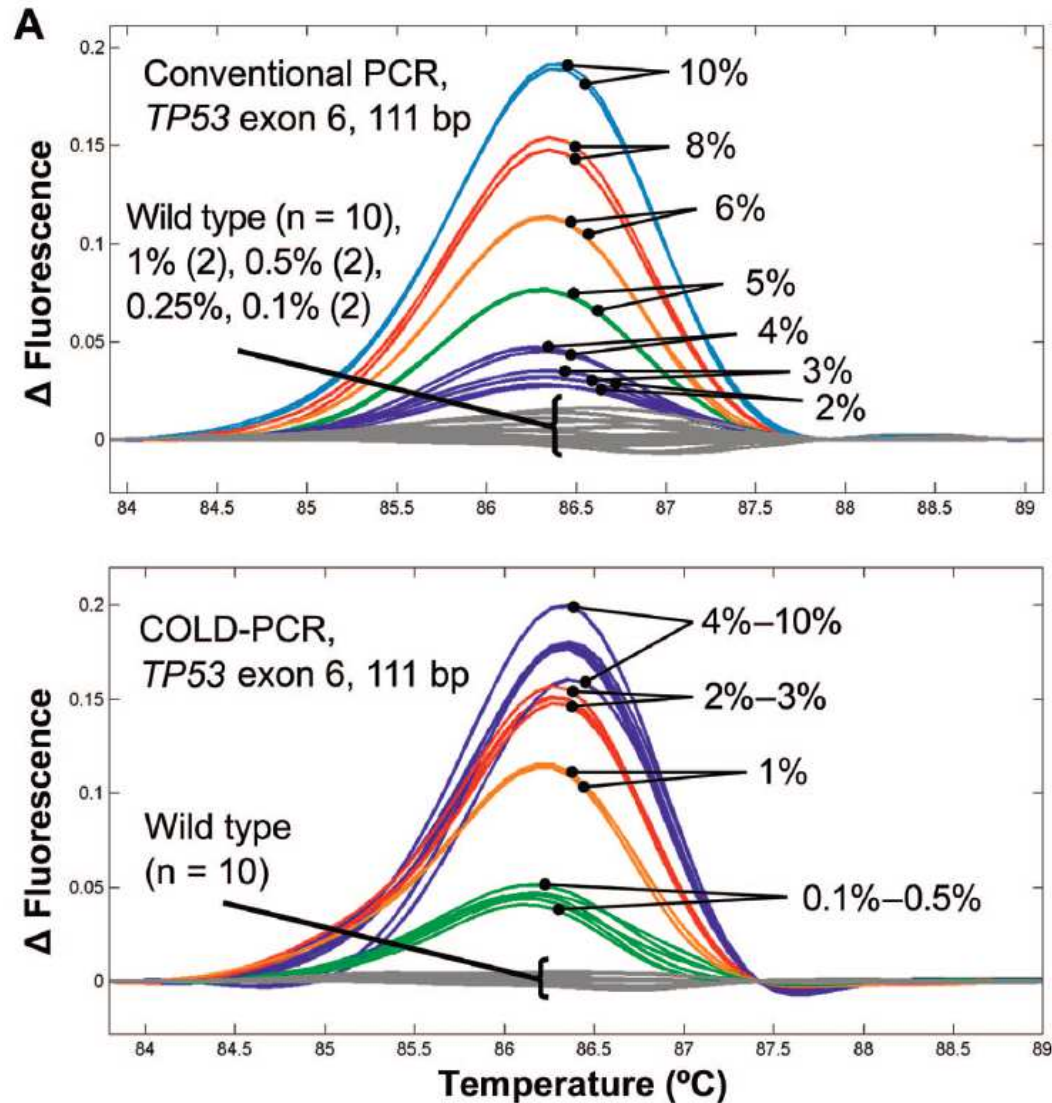


High Resolution Melting Analysis (HRMA)



SNP Class	Base Change	Typical T _m Shift	Rarity (in human genome)
1	C/T and G/A	Large (>0.5°C)	64%
2	C/A and G/T		20%
3	C/G	Very Small (<0.2°C)	9%
4	A/T		7%

COLD-PCR with HRMA



COLD-PCR with RFLP (Sudha's results)

- a. First step: COLD-PCR with 0.1X LC Green as described above (point 5).
- b. Second step: Regular PCR with 1X LC Green, using
 - Primer pair: A1-A2
 - Template DNA: 1:1000 dilution of the product from first step
 - Cycling conditions:
 - 95°C; 120secs
 - 95°C; 15secs
 - 55°C; 30secs, plate read
 - 72°C; 1min
 - GOTO step 2 30 times
 - Melt Curve@ 65°C to 98°C at 0.2°C/sec with a 10sec hold.

@: melt curve conditions used as recommended by BioRad.

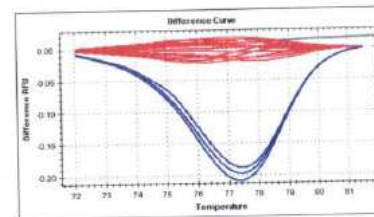
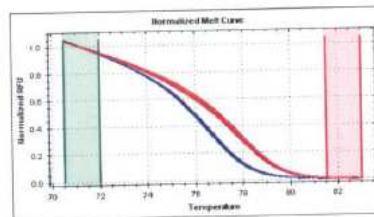
Observations:

1. When checked on a gel the COLD-PCR products as well as the Rd2 Reg PCR products only show smears. According to Ref 1, T_c is the lowest denaturing temperature that reproducibly yields a substantial product. The authors state that the temperature selected as T_c is usually below the T_m of WT, mutant or mismatched sequences.

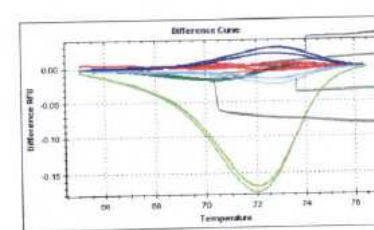
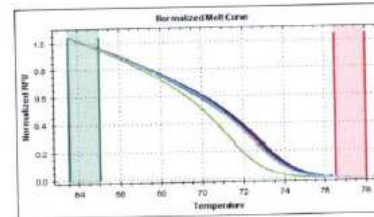
COLD-PCR with HRMA (Sudha's results)

Melt in Benzyl Trimethylammonium Chloride (BTriMAC) (0.1-0.5M)

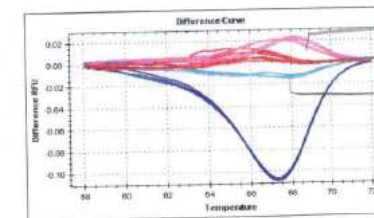
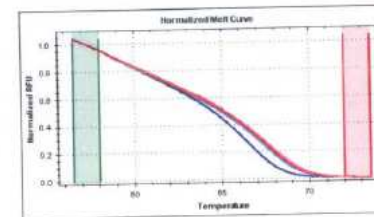
No solvt
90/0.1



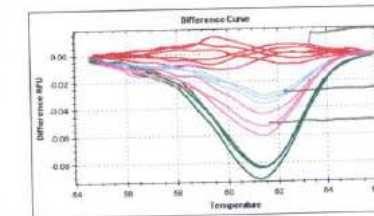
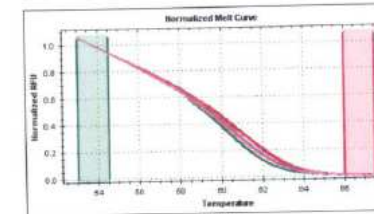
0.1M BTriMAC
90/0.1



0.25M BTriMAC
90/0.1



0.5M BTriMAC
90/0.1



COLD-PCR Clinical application 1

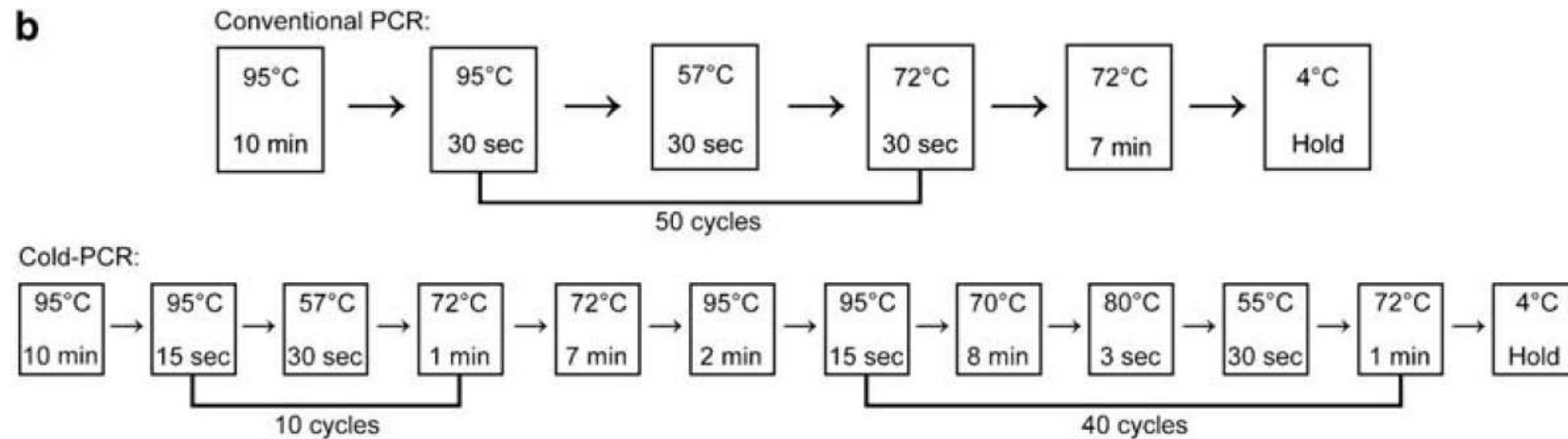
Application of COLD-PCR for improved detection of *KRAS* mutations in clinical samples

KRAS mutations have been detected in approximately 30% of all human tumors, and have been shown to predict response to some targeted therapies. The most common *KRAS* mutation-detection strategy consists of conventional PCR and direct sequencing. This approach has a 10–20% detection sensitivity depending on whether pyrosequencing or Sanger sequencing is used. To improve detection sensitivity, we compared our conventional method with the recently described co-amplification-at-lower denaturation-temperature PCR (COLD-PCR) method, which selectively amplifies minority alleles. In COLD-PCR, the critical denaturation temperature is lowered to 80°C (vs 94°C in conventional PCR). The sensitivity of COLD-PCR was determined by assessing serial dilutions. Fifty clinical samples were used, including 20 fresh bone-marrow aspirate specimens and the formalin-fixed paraffin-embedded (FFPE) tissue of 30 solid tumors. Implementation of COLD-PCR was straightforward and required no additional cost for reagents or instruments. The method was specific and reproducible. COLD-PCR successfully detected mutations in all samples that were positive by conventional PCR, and enhanced the mutant-to-wild-type ratio by > 4.74-fold, increasing the mutation detection sensitivity to 1.5%. The enhancement of mutation detection by COLD-PCR inversely correlated with the tumor-cell percentage in a sample. In conclusion, we validated the utility and superior sensitivity of COLD-PCR for detecting *KRAS* mutations in a variety of hematopoietic and solid tumors using either fresh or fixed, paraffin-embedded tissue.

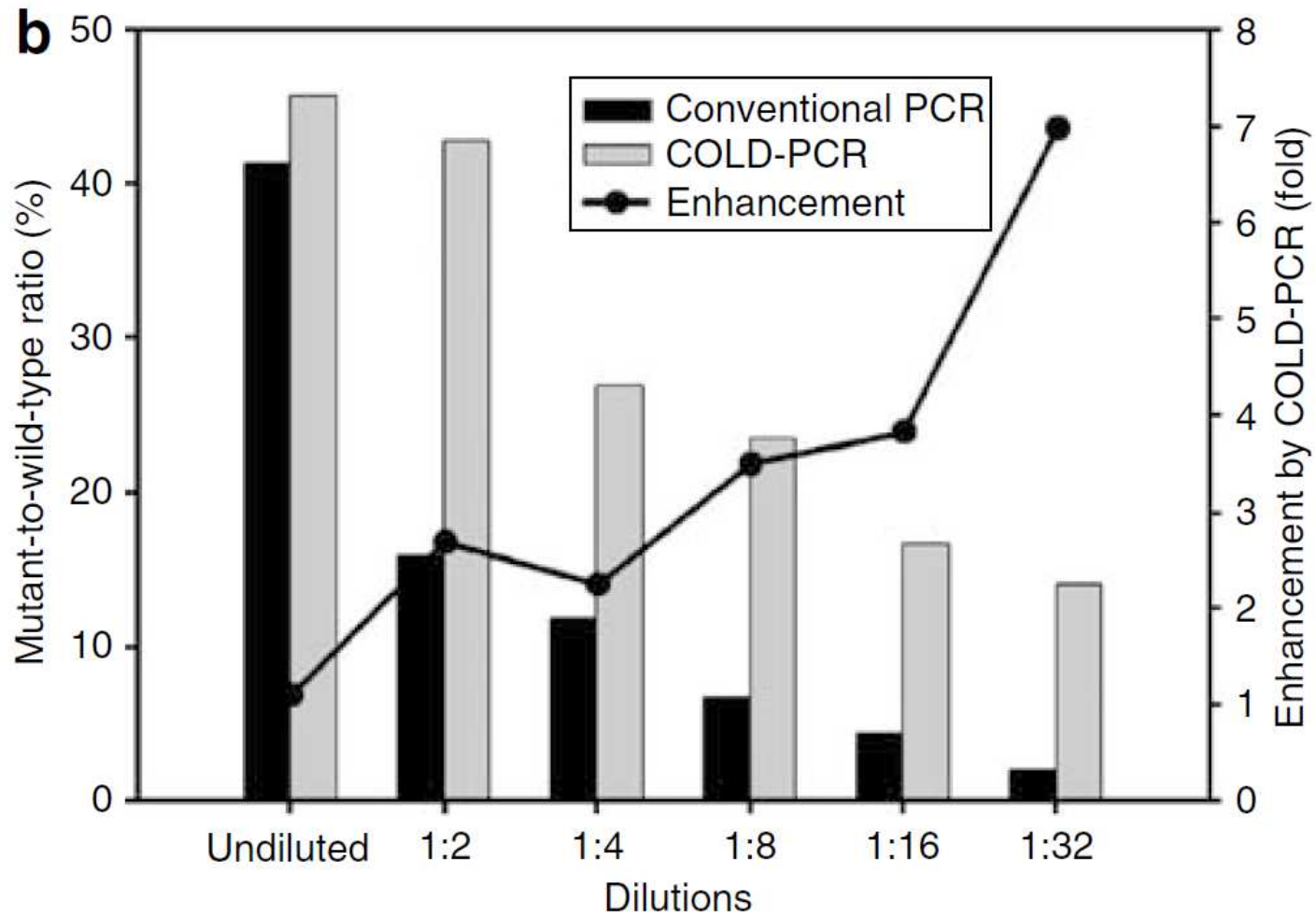
Modern Pathology (2009) 22, 1023–1031; doi:10.1038/modpathol.2009.59; published online 8 May 2009

COLD-PCR Clinical application 1

b



COLD-PCR Clinical application 1



COLD-PCR Clinical application 1

Table 2 Comparison of mutant-to-wild-type-ratio by conventional PCR and COLD-PCR in fresh bone-marrow aspirate samples

No.	Age	Diagnosis (FAB classification)	Mutation type	Nucleotide change	Tumor cell count (%)	Ratio by conventional PCR (%) ^a	Ratio by COLD-PCR (%)	Enhancement by COLD- PCR (fold)
1	57	MDS	G12D	GGT to GAT	4	1.7	1.8	1.0
2	84	AML (M2)	G12D	GGT to GAT	31	23.7	55.3	2.3
3	48	MDS	G13S	GGC to AGC	2	6.2	12.1	1.9
4	33	AML	G12V	GGT to GTT	83	28.9	51.6	1.8
5	63	MDS	G12S	GGT to AGT	4	57.7	67.7	1.2
6	60	AML (M4)	G12D	GGT to GAT	52	2.4	3.1	1.3
7	50	AML (M2)	G12D	GGT to GAT	40	47.2	66.0	1.4
8	57	CMML	G12D	GGT to GAT	10	64.1	68.0	1.1
9	35	AML (M5)	G12V	GGT to GTT	75	39.4	57.0	1.5
10	51	AML	G12D	GGT to GAT	36	20.7	31.2	1.5
11	31	AML (M5)	G12D	GGT to GAT	80	19.7	23.3	1.2
12	78	CMML	G12R	GGT to CGT	14	50.3	54.5	1.1
13	78	AML	G12D	GGT to GAT	90	44.7	40.6	0.9
14	72	MDS	G12R	GGT to CGT	8	16.5	21.9	1.3
15	77	MDS	G12R	GGT to CGT	80	32.5	35.0	1.1
16	79	AML (M4)	G12D	GGT to GAT	35	24.7	38.8	1.6
48	49	AML (M2)	G12D	GGT to GAT	3	0.0	8.1	

AML, acute myeloid leukemia; CMML, chronic myelomonocytic leukemia; COLD-PCR, co-amplification-at-lower denaturation-temperature PCR; MDS, myelodysplastic syndrome.

^aMean tumor cell count = 38.06%.

COLD-PCR Clinical application 2

Potential clinical significance of plasma-based KRAS mutation analysis using the COLD-PCR/TaqMan[®]-MGB probe genotyping method

Abstract. Despite the improved ability to detect mutations in recent years, tissue specimens cannot always be procured in a clinical setting, particularly from patients with recurrence of tumors or metastasis. Therefore, the aim of this study was to investigate whether plasma is able to be used for mutation analysis instead of tissue specimens. We collected plasma from 62 patients with colorectal cancer (CRC) prior to treatment. DNA extracted from plasma and matched tumor tissues were obtained. Mutations in KRAS were amplified from the tissue specimens and sequenced by regular polymerase chain reaction (PCR) and co-amplification at lower denaturation temperature (COLD)-PCR. Plasma KRAS gene mutation on codon 12 (GGT>GAT) was detected using a nested COLD-PCR/TaqMan[®]-MGB probe. Mutations in plasma and matched tumors were compared. KRAS mutation on codon 12 (GGT>GAT) was found in 13 (21.0%) plasma specimens and 12 (19.4%) matched tumor tissues. The consistency of KRAS mutations between plasma and tumors was 75% (9/12), which indicated a high correlation between the mutations detected in plasma DNA and the mutations detected in the corresponding tumor DNA ($P<0.001$; correla-

tion index, $k=0.649$). Notably, four (6.5%) patients with plasma DNA mutations had no detectable KRAS mutations in the corresponding primary tumors, and three (4.8%) patients with tumor DNA mutations had no detectable KRAS mutations in the corresponding plasma DNA samples. Thus, KRAS mutations in plasma DNA correlate with the mutation status in matched tumor tissues of patients with CRC. Our study provides evidence to suggest that plasma DNA may be used as a potential medium for KRAS mutation analysis in CRC using the COLD-PCR/TaqMan-MGB probe method.

COLD-PCR Clinical application 3

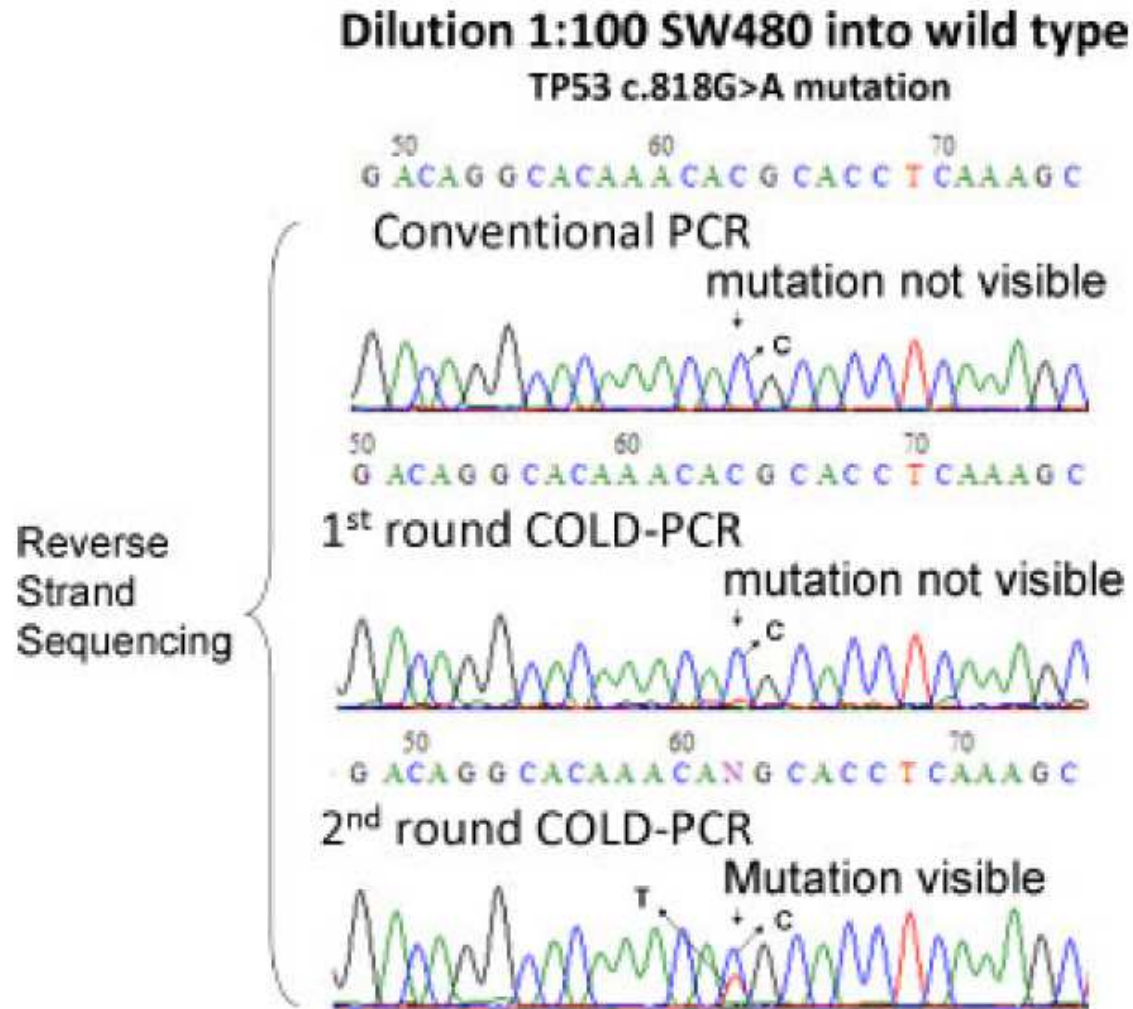
Two-Round Coamplification at Lower Denaturation Temperature–PCR (COLD-PCR)-Based Sanger Sequencing Identifies a Novel Spectrum of Low-Level Mutations in Lung Adenocarcinoma

ABSTRACT: Reliable identification of cancer-related mutations in TP53 is often problematic, as these mutations can be randomly distributed throughout numerous codons and their relative abundance in clinical samples can fall below the sensitivity limits of conventional sequencing. To ensure the highest sensitivity in mutation detection, we adapted the recently described coamplification at lower denaturation temperature–PCR (COLD-PCR) method to employ two consecutive rounds of COLD-PCR followed by Sanger sequencing. Using this highly sensitive approach we screened 48 nonmicrodissected lung adenocarcinoma samples for TP53 mutations. Twenty-four missense/frameshift TP53 mutations throughout exons 5 to 8 were identified in 23 out of 48 (48%) lung adenocarcinoma samples examined, including eight low-level mutations at an abundance of ~1 to 17%, most of which would have been missed using conventional methodologies. The identified alterations

include two rare lung adenocarcinoma mutations, one of which is a “disruptive” mutation currently undocumented in the lung cancer mutation databases. A sample harboring a low-level mutation (~2% abundance) concurrently with a clonal mutation (80% abundance) revealed intratumoral TP53 mutation heterogeneity. The ability to identify and sequence low-level mutations in the absence of elaborate microdissection, via COLD-PCR-based Sanger sequencing, provides a platform for accurate mutation profiling in clinical specimens and the use of TP53 as a prognostic/predictive biomarker, evaluation of cancer risk, recurrence, and further understanding of cancer biology.

Hum Mutat 30:1583–1590, 2009. © 2009 Wiley-Liss, Inc.

COLD-PCR Clinical application 3



COLD-PCR Clinical application 3

Table 1. TP53 Mutations Identified Via Two-Round COLD-PCR-Based Sanger Sequencing*

Samples	Mutation (nt)	Mutation (aa)	Detectable via conventional PCR – Sanger sequencing ^b	Independent confirmation ^c	Mutation abundance (%)
TL96	c.747G>T	p.Arg249Ser	No	R, P	6.7
TL121	c.733G>A	p.Gly245Ser	No	R, P	7
TL119	c.730G>T	p.Gly244Cys	No	R, P	7.5
TL6 ^a	c.830G>T	p.Cys277Phe	No	R	~2–3
TL8	c.853G>T	p.Glu285X	No	R	~1–2
TL82	c.811G>A	p.Glu271Lys	No	R, P	11
TL135	c.646G>A	p.Val216Met	No	P	17
TL22	c.469G>T	p.Val157Phe	No	P	16.6
TL134	c.733G>T	p.Gly245Cys	Yes	–	~45
TL125	c.742C>T	p.Arg248Trp	Yes	–	~90
TL15	c.818G>A	p.Arg273His	Yes	–	~40
TL123	c.810_819del	p.Phe270fs	Yes	–	~50
TL14	c.844C>G	p.Arg282Gly	Yes	–	~60
TL18	c.839G>A	p.Arg280Lys	Yes	–	~70
TL92	c.845del	p.Arg282fs	Yes	–	~50
TL124	c.809_818del	p.Phe270fs	Yes	–	~60
TL5	c.830G>T	p.Cys277Phe	Yes	–	~37
TL136	c.601_602del	p.Leu201fs	Yes	–	~80
TL106	c.460del	p.Gly154fs	Yes	–	~70
TL107	c.461G>T	p.Gly154Val	Yes	–	~33
TL112	c.473G>T	p.Arg158Leu	Yes	–	~50
TL117	c.388C>G	p.Leu130Val	Yes	–	~80
TL6 ^a	c.589G>A	p.Val197Met	Yes	–	~80
TL97	c.743G>T	p.Arg248Leu	Yes	–	~40

*Reference sequence used for the TP53 gene was RefSeq NM_000546.4. Nucleotide numbering reflects cDNA numbering with +1 corresponding to the A of the ATG translation initiation codon in the reference sequence. The initiation codon is codon 1.

^aTwo concurrent mutations in a single sample.

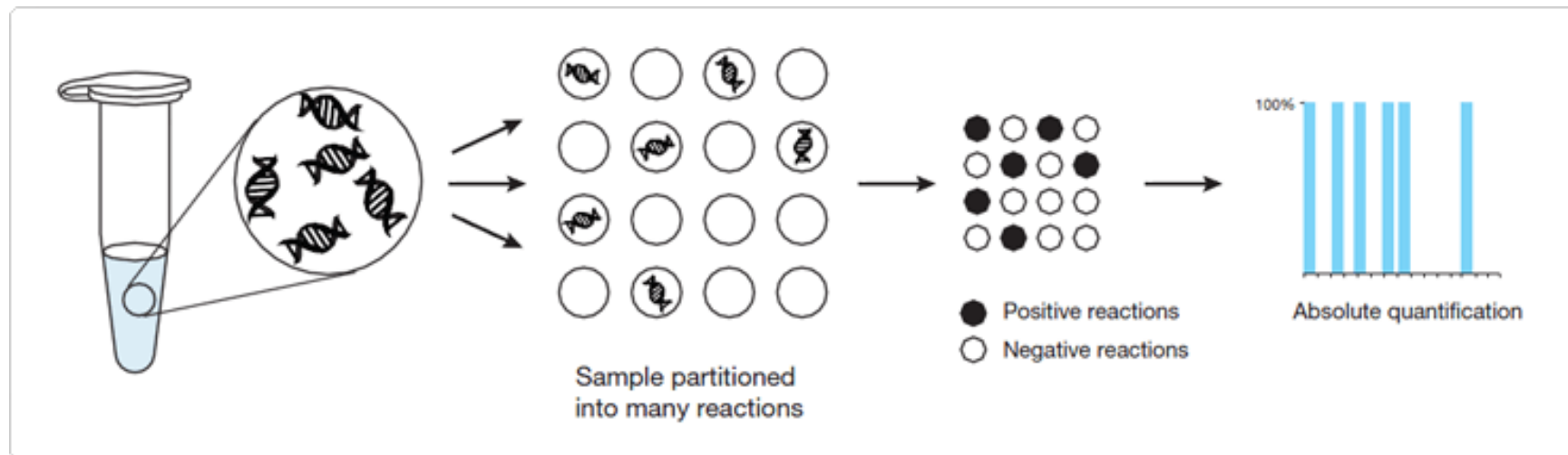
^bFor mutations detectable via conventional PCR-Sanger sequencing, no independent confirmation was provided.

^cR and P represent independent confirmation by RFLP, pyrosequencing, respectively.

COLD-PCR alternatives

Method	Selectivity	Description	Disadvantages compared to COLD-PCR
Enrichment of known mutations			
Amplification refractory mutation system (ARMS)	10^{-1} to 10^{-3}	Relies on <u>known</u> 3' end variation to enrich allele-specific PCR	Mutation must be known in advance for specific primer design
Allele specific PCR (ASPCR)	10^{-1} to 10^{-3}	Use of a primer that will only amplify the <u>known</u> mutation	Mutation must be known in advance for specific primer design
Restriction site mutation assay PCR (RSM-PCR)	10^{-3} to 10^{-8}	Use nuclease that selectively digests WT allele – leaving only variant for PCR enrichment.	Variant allele must be known and result in restriction site
Digital PCR and Random mutation capture PCR (RMC-PCR)	10^{-3} to 10^{-8}	Isolation of individual DNA molecules for PCR. Can potentially isolate single variant DNA sequence.	Requires specific and expensive machinery and mutations must be known in advance
Enrichment of unknown mutations			
Electrophoresis (i.e. Denaturing-High Performance liquid chromatography)	10^{-1} to 10^{-2}	Uses physical differences in homo- and heteroduplex DNA to separate WT and variants	Requires specific and sometimes expensive machinery. Adds extra PCR steps before and after separation experiment
Inverse PCR-based amplified RFLP (iFLP)	10^{-3} to 10^{-5}	Variant DNA that results in TaqI sites is linearized, ligated to linkers, and amplified. WT DNA is not.	Only targets the 3-5% of mutations that result in TaqI restriction sites

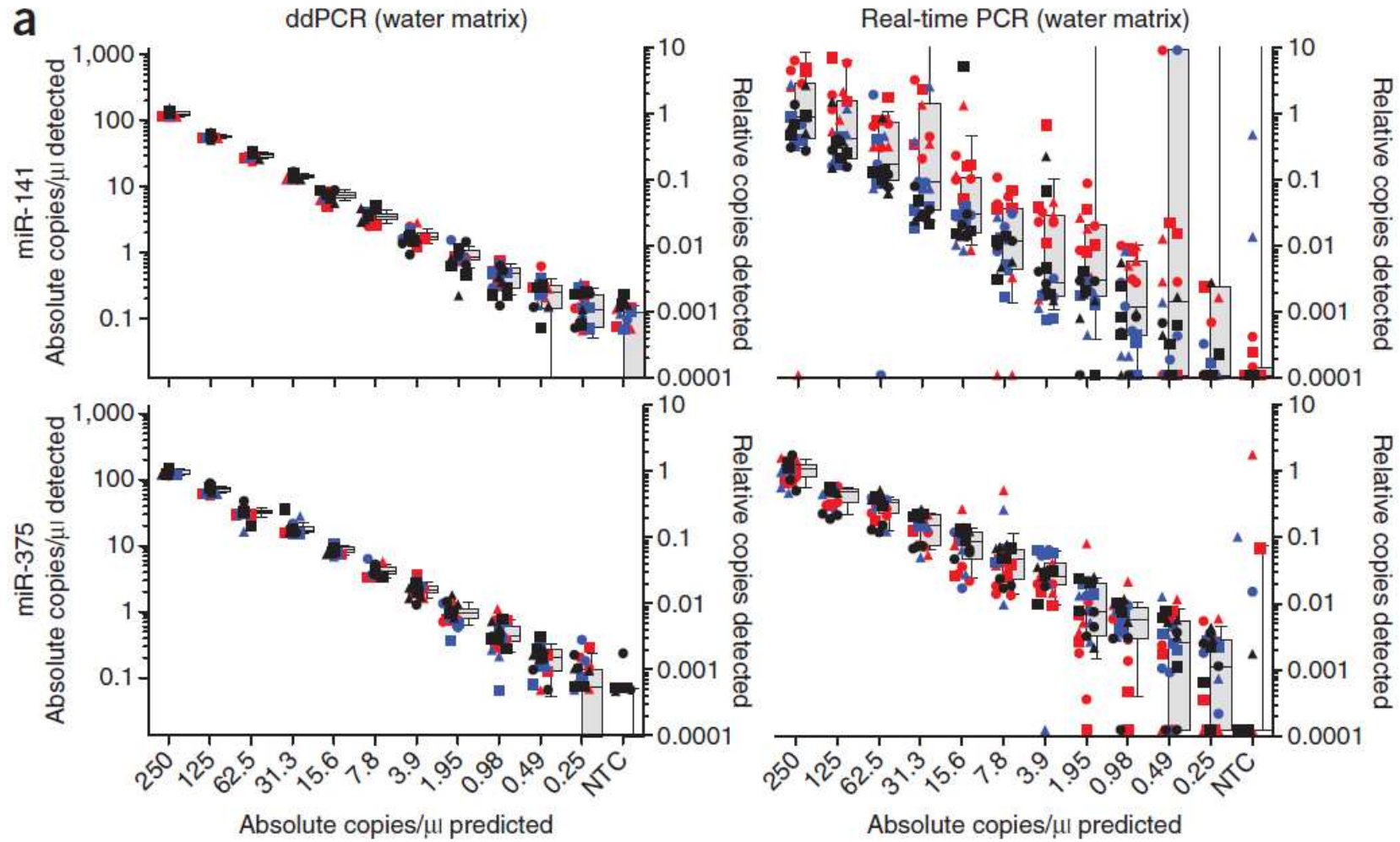
Digital PCR: how it works



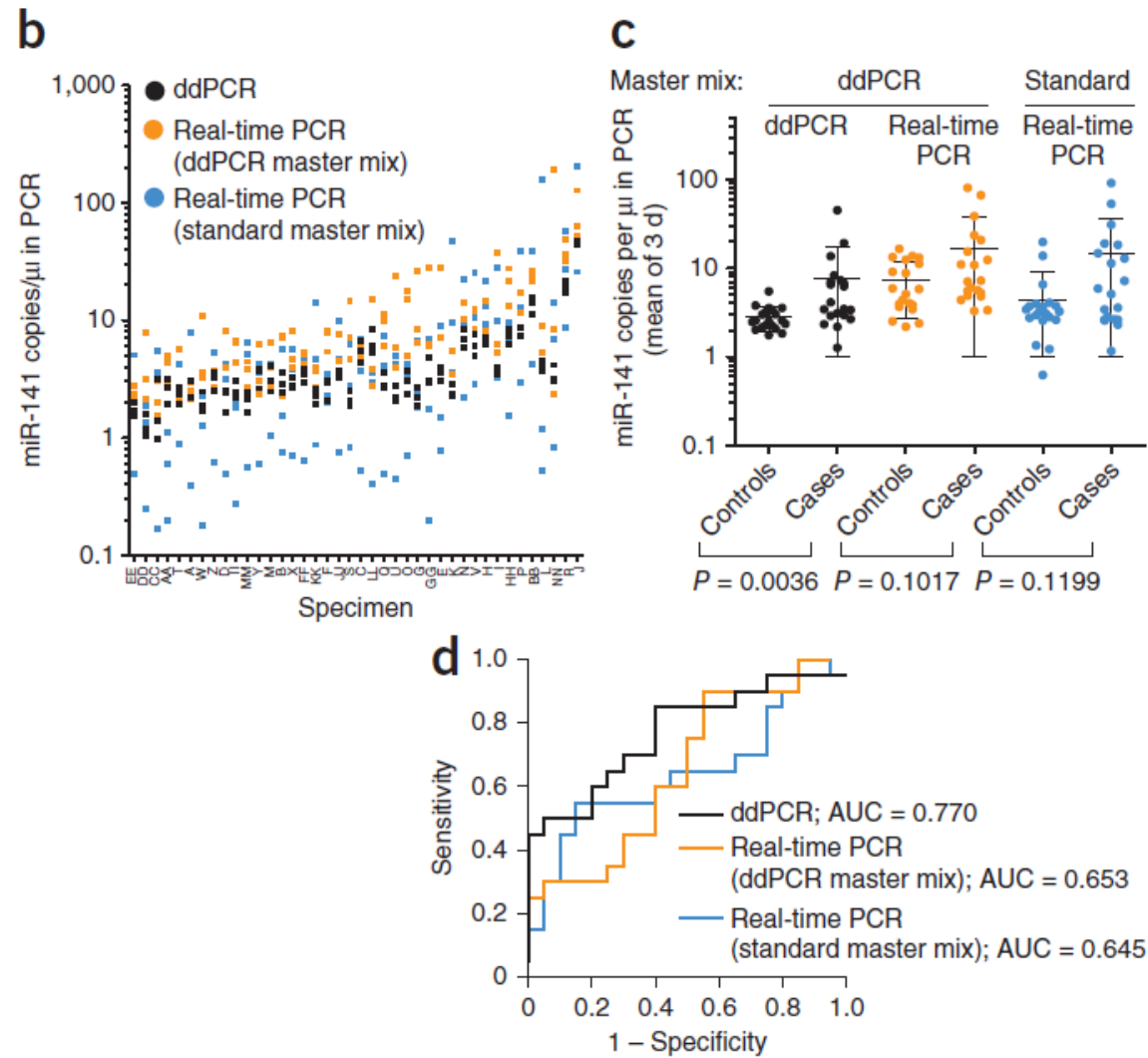
qPCR Vs. Digital PCR

Specification	Real-Time PCR	Digital PCR
Dynamic Range	Broad	Low-Medium
Specificity	.1% using castPCR	1% or better
Sensitivity	1 copy/reaction	1 copy/ml
Precision	Measure differences up to 4 and 5 copies	Measure differences over 4 and 5 copies
Applications	Gene Expression	GMO Contamination Detection
	Genotyping	Quantitation of Viral Load
	Copy Number Analysis	Generating References and Standards
	Micro RNA & Non-coding RNA Analysis	Rare Target Detection

qPCR Vs. Digital PCR



qPCR Vs. Digital PCR



Digital PCR: Instrumentation

Table 1 | Commercial digital PCR offerings

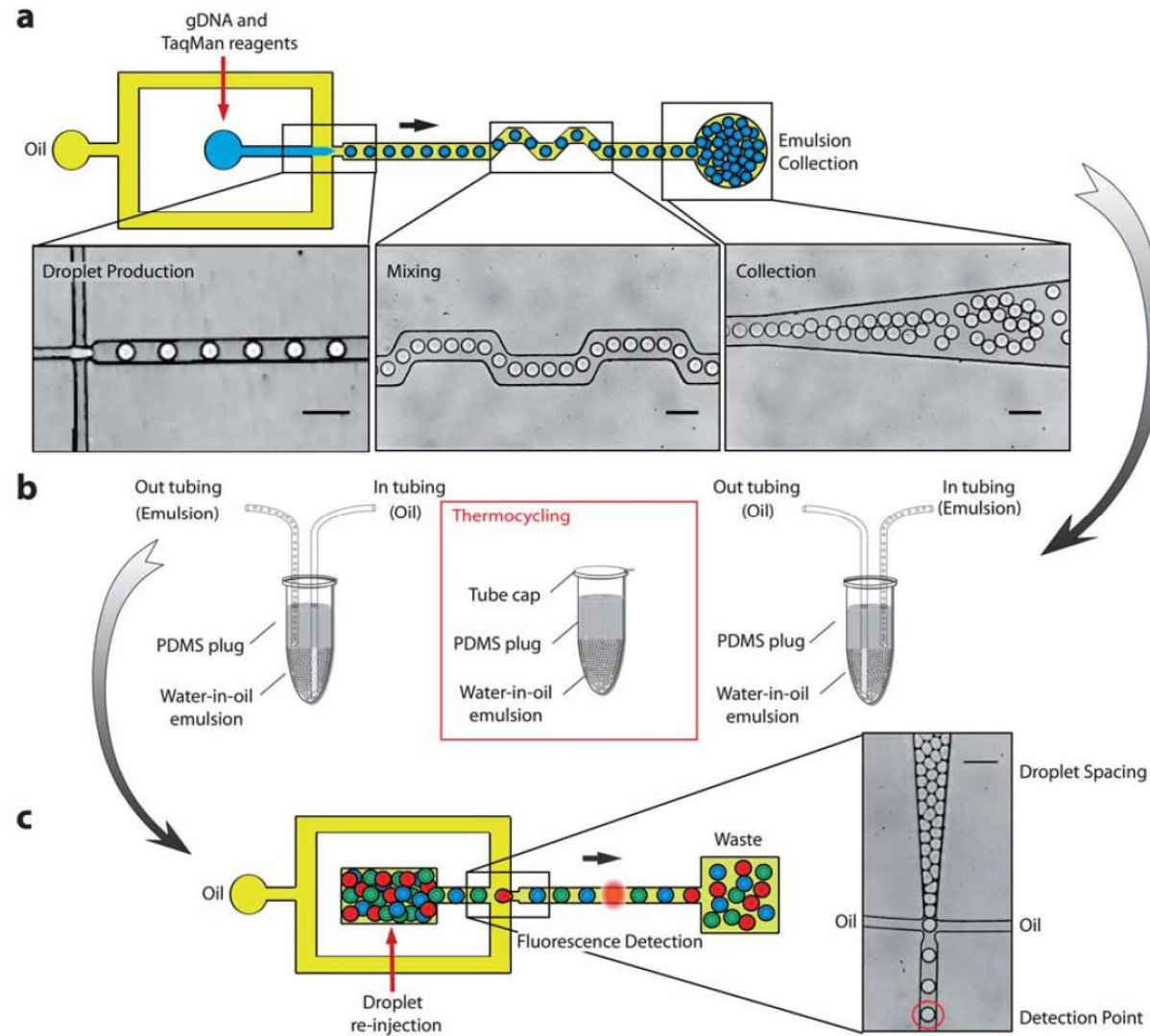
Vendor	Instruments and list price	Consumables and list price	Number and volume of partitions	Volumes required	qPCR capacity	Multiplexing
Fluidigm Corporation	BioMark HD: \$200,000–\$250,000	12 arrays per chip ^a (765 wells per array): \$400 per chip (works in both EP1 and BioMark)	12-inlet chip: 9,180 partitions, 6 nl per partition	12-inlet chip: 8 µl of mix, ~4 µl of sample; 57% analyzed ^b	Yes	Can use up to 5 colors to detect 5 targets (assumes 5th color is ultraviolet)
	EP1: \$100,000–\$150,000	48 arrays per chip ^a (770 wells per array): \$800 per chip (works in both EP1 and BioMark)	48-inlet chip: 36,960 partitions, 0.85 nl per partition	48-inlet chip: 4 µl of mix, ~2 µl of sample ^b	No	Can use up to 5 colors to detect 5 targets
Life Technologies	OpenArray RealTime PCR System and QuantStudio 12K Flex instrument: \$140,000 and \$90,000–\$190,000, respectively	OpenArray plates ^a (64 holes per subarray): \$150 per plate	Varies; 3,072 partitions per plate, 48 subarrays per plate, 33 nl per partition (machines run 3–4 plates at once)	100 µl of sample per plate (across 48 arrays)	Yes	Uses 2 colors of probes to detect 2 targets
Bio-Rad Laboratories	QX100 ddPCR System (machines to generate and read droplets): \$89,000	8 samples per chip (14,000–16,000 droplets per sample): \$3 per sample	Up to 96 samples per run (assumes manual pipetting into PCR plate); 1,344,000 partitions per run (assuming separate thermocycler runs 12 chips at once), 1 nl per partition	Up to 9 µl per sample (20,000 droplets made); an average of 70% read	No	Uses 2 colors to detect 2 targets
RainDance ^c	RainDrop Digital PCR (machines to generate, collect and read droplets): \$100,000	8 samples per chip (up to 10,000,000 droplets per sample): \$10–\$30 per sample	8 samples per run; up to 80,000,000 partitions per run, 5 pl per partition	5–50 µl per sample	No	Uses 2 colors, but can use varying concentrations of probes to detect up to 10 targets

^aArrays can hold separate samples, or the same sample can be spread over multiple arrays. ^bFor rare allele analysis, protocols are available to eliminate the dead volume. ^cPlans full commercial launch later this year.

Digital PCR: Enzyme concentration

- 1U enzyme $\sim 2 \times 10^{-4}$ nmol.
- 5U enzyme in 200 μ L reaction $\sim 5 \times 10^{-9}$ nmol/nL.
- For BioRad ddPCR: 1 nL per droplet.
- So $\sim 5 \times 10^{-18}$ mol, or 2.5×10^{-5} , or 3×10^6 molecules of enzymes in one droplet.

Droplet-based digital PCR



Droplet-based digital PCR

- Detection of KRAS mutation among 200,000 fold excessive wt background

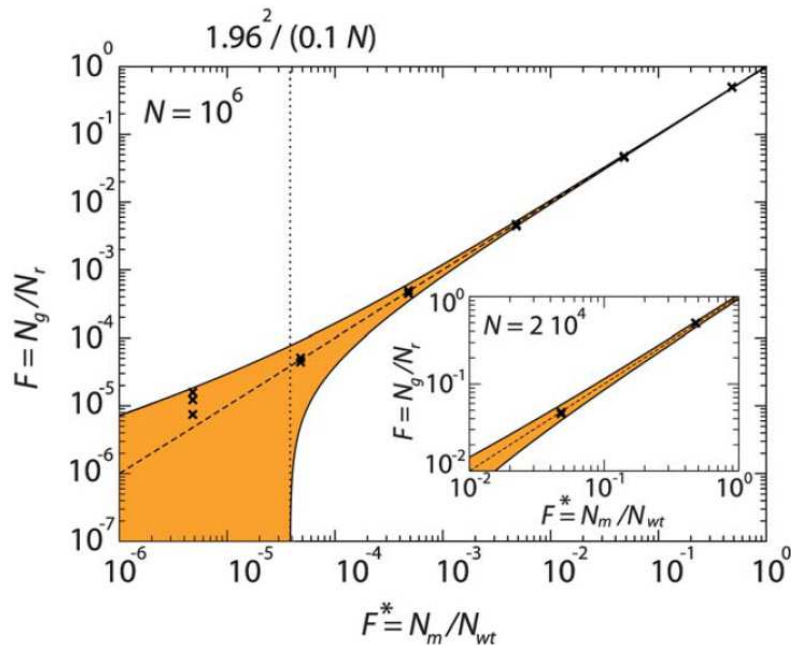
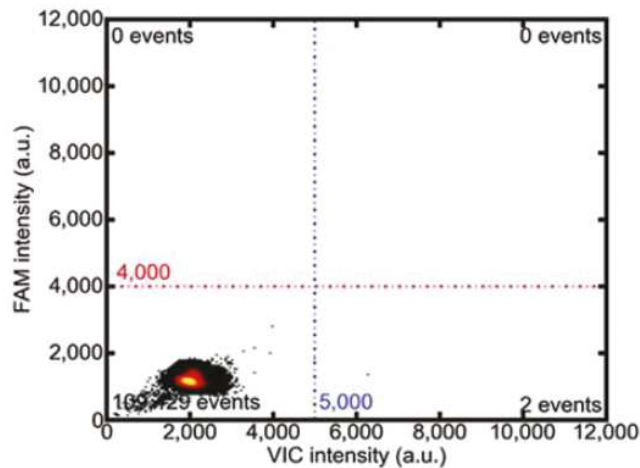


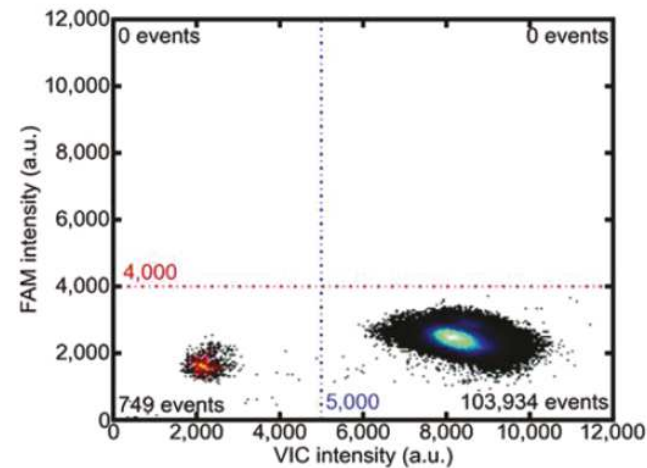
Fig. 3 Sensitivity of the method. Experimental measurement of the fraction of green-fluorescent droplets containing mutant *KRAS* (N_g) over the number of red-fluorescent droplets containing wild-type *KRAS* (N_r) as a function of the ratio of mutant (N_m) to wild-type (N_{wt}) genes. In an ideal assay, N_g/N_r is equal to N_m/N_{wt} (dashed line). The 95% confidence interval (orange area) for the analysis of $N = 10^6$ droplets when $N_{wt}/N = 0.1$ is shown (see ESI† for details on the determination of the 95% confidence interval). All the experimental points (\times) obtained in duplicate (except for the 1/200 000 which was in triplicate) for the different dilutions fall into this 95% confidence interval. The dotted line corresponds to the point where a measured $N_m = 0$ falls in the 95% confidence interval. Inset: higher ratios of mutant to wild-type genes, statistically relevant data are obtained by the analysis of a smaller subset of droplets. The experimental points (\times) are plotted as a zoom and compared to the 95% confidence interval (orange area) determined from the analysis of $N = 2 \times 10^4$ droplets analyzed experimentally.

Digital PCR: rare allele detection

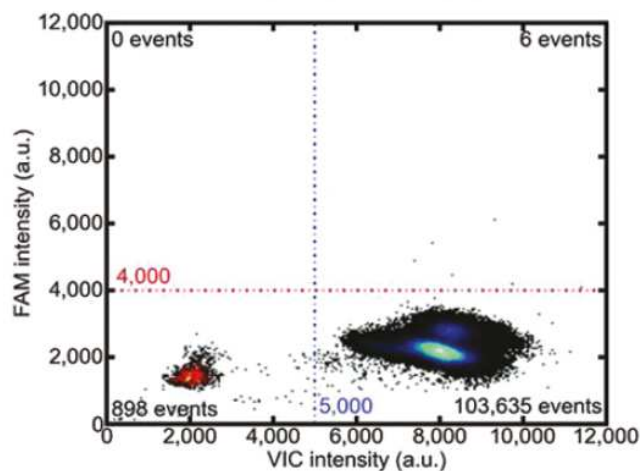
No template control



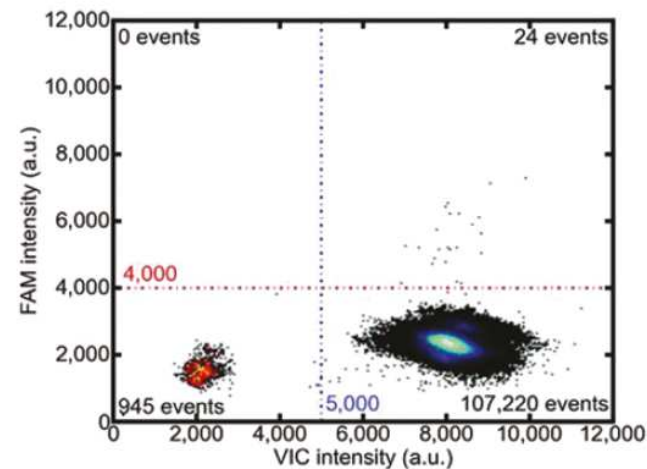
0% mutant (wildtype only)



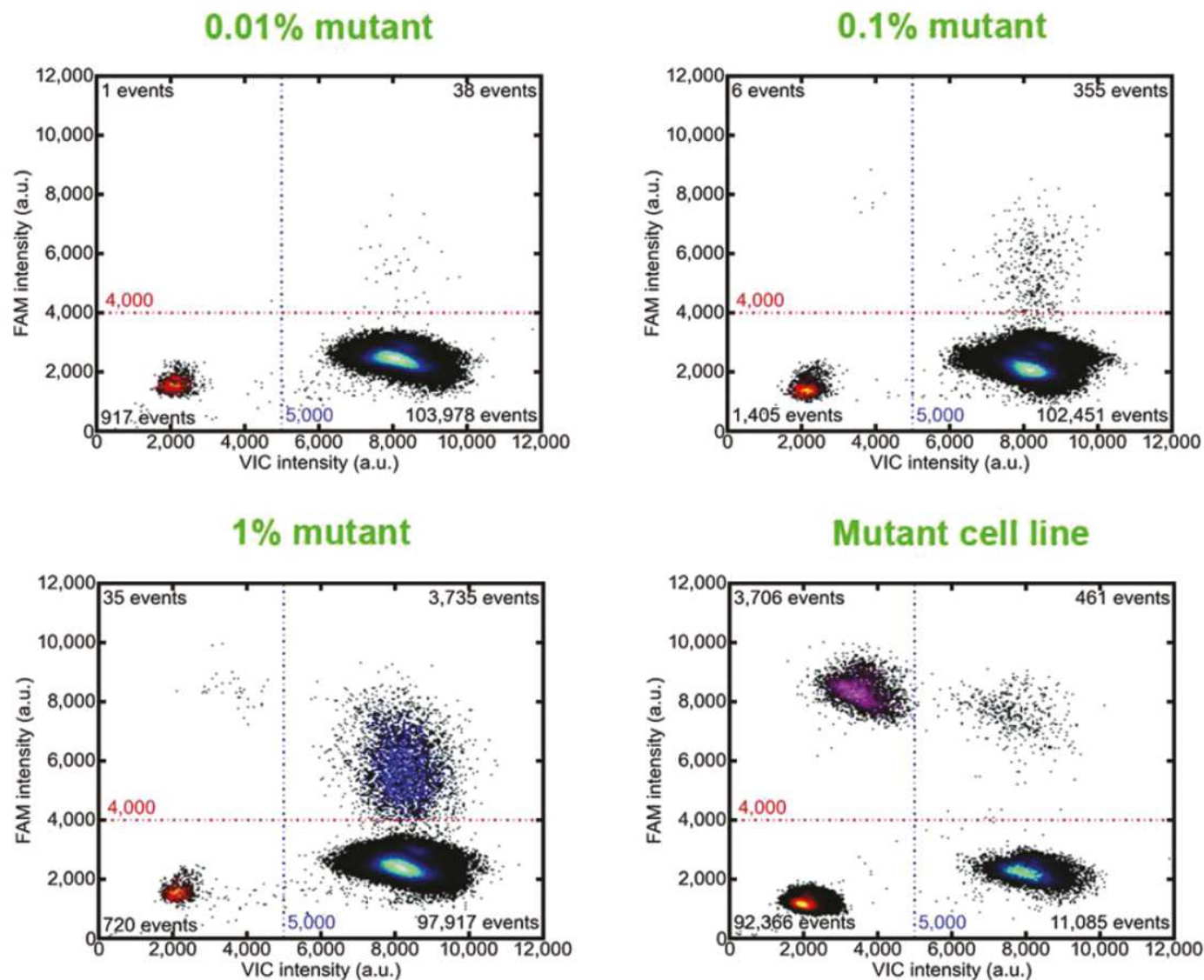
0.001% mutant



0.005% mutant



Digital PCR: rare allele detection (con't)



Digital PCR: clinical application

- Non-invasive pre-natal diagnosis
- Quantification of viral DNA
- Detection of rare allele
- Detection of mutants in free circulating DNA

Digital PCR: clinical application 1

Multiplex Picodroplet Digital PCR to Detect *KRAS* Mutations in Circulating DNA from the Plasma of Colorectal Cancer Patients

BACKGROUND: Multiplex digital PCR (dPCR) enables noninvasive and sensitive detection of circulating tumor DNA with performance unachievable by current molecular-detection approaches. Furthermore, picodroplet dPCR facilitates simultaneous screening for multiple mutations from the same sample.

METHODS: We investigated the utility of multiplex dPCR to screen for the 7 most common mutations in codons 12 and 13 of the *KRAS* (Kirsten rat sarcoma viral oncogene homolog) oncogene from plasma samples of patients with metastatic colorectal cancer. Fifty plasma samples were tested from patients for whom the primary tumor biopsy tissue DNA had been characterized by quantitative PCR.

RESULTS: Tumor characterization revealed that 19 patient tumors had *KRAS* mutations. Multiplex dPCR analysis of the plasma DNA prepared from these samples identified 14 samples that matched the mutation identified in the tumor, 1 sample contained a different *KRAS* mutation, and 4 samples had no detectable mutation. Among the tumors samples that were wild type for *KRAS*, 2 *KRAS* mutations were identified in the corresponding plasma samples. Duplex dPCR (i.e., wild-type and single-mutation assay) was also used to analyze plasma samples from patients with *KRAS*-mutated tumors and 5 samples expected to contain the *BRAF* (v-raf murine sarcoma viral oncogene homolog B) V600E mutation. The results for the duplex analysis matched those for the multiplex analysis for *KRAS*-mutated samples and, owing to its higher sensitivity, enabled detection of 2 additional samples with low levels of *KRAS*-mutated DNA. All 5 samples with *BRAF* mutations were detected.

Digital PCR: clinical application 1

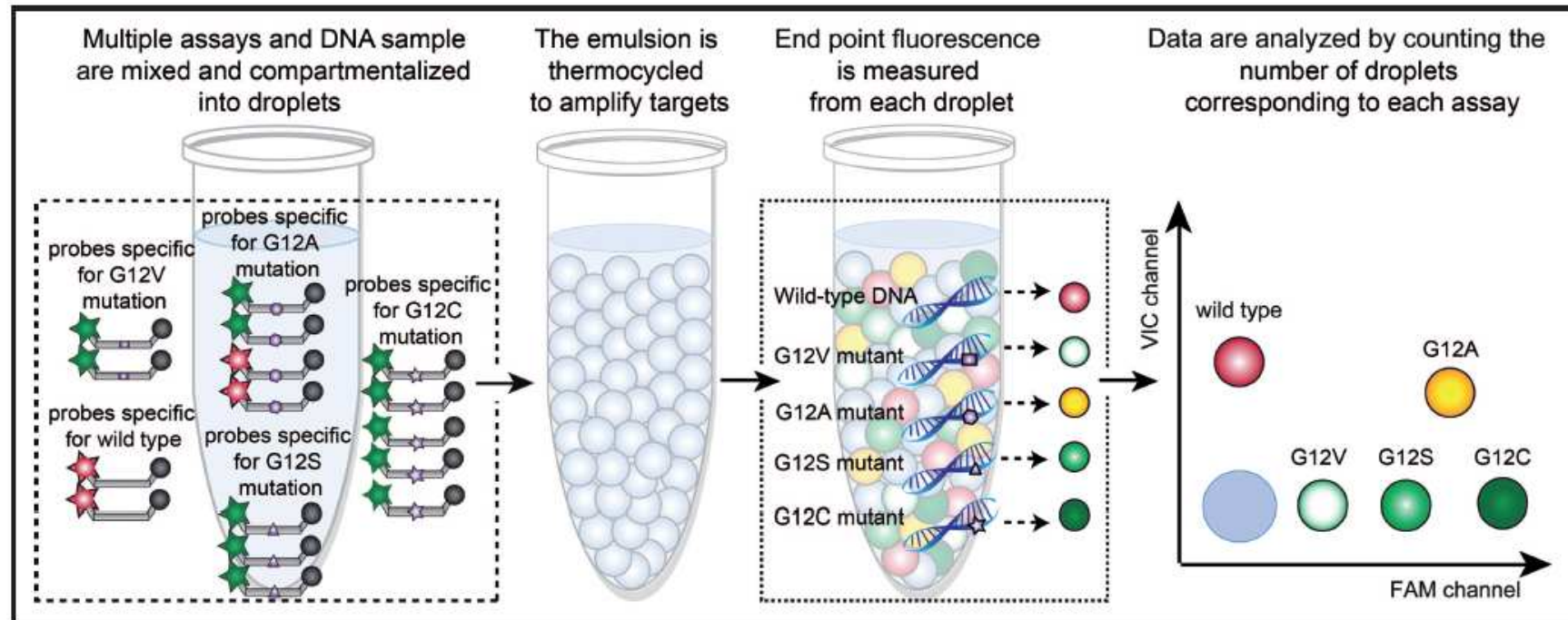


Fig. 1. Multiplex analysis of circulating tumor DNA: example of the 5-plex assay.

An aqueous phase containing TaqMan[®] assay reagents and genomic DNA is emulsified. Probes specific for the 4 screened mutations and the wild-type sequence are present at varying concentrations. After thermal cycling the droplets' end point fluorescence depends on the initial concentration of the probes, allowing the identification of the target sequences.

Digital PCR: clinical application 1

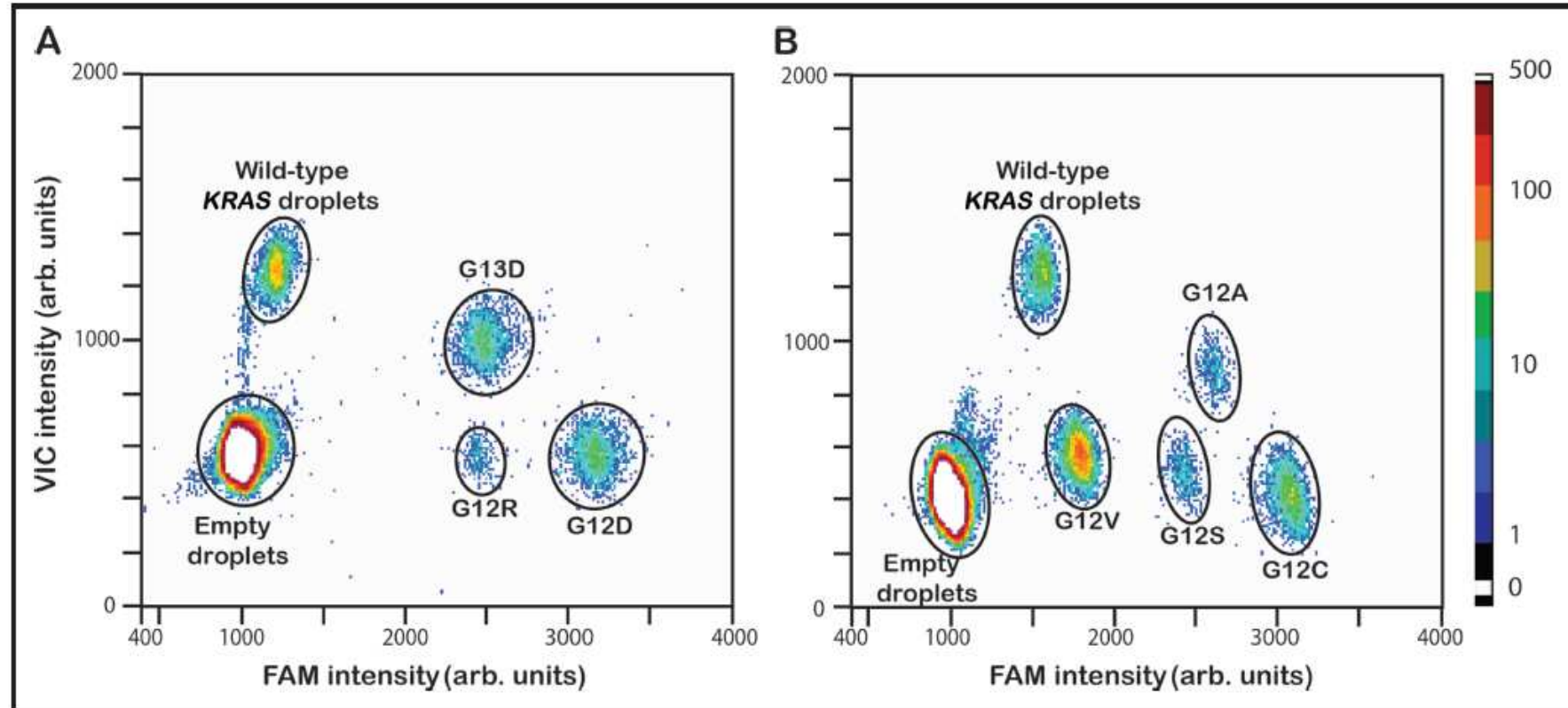


Fig. 2. Multiplex assays for mutant *KRAS* analysis. Two-dimensional histogram of the 4-plex (A) and the 5-plex assay (B). Fragmented genomic DNA extracted from cell lines was encapsulated in droplets and submitted to the procedure described in Fig. 1. FAM, 6-carboxyfluorescein; arb. units, arbitrary units.

Digital PCR: clinical application 1

Table 1. Duplex and multiplex analysis of plasma samples of patients with *KRAS*- or *BRAF*-mutated primary tumor.^a

Sample	Concentration, ng/mL of plasma	Tumor mutation	Multiplex <i>KRAS</i> analysis		Duplex <i>KRAS</i> analysis	
			Mutation	Mutant DNA, %	Mutation	Mutant DNA, %
1	12	G12D	G12D	0.65	G12D	0.59
4	24	G12D	G12D	2.52	G12D	5.81
7	14	G12D	NM ^b	—	G12D	0.17
8	53	G12C	G12C	0.16	G12C	0.18
9	201	G12A	G12A	24.09	G12A	24.79
10	89	G13D	G13D	42.99	G13D	45.78
11	1466	G12D	G12D	0.53	G12D	0.57
13	32	G13D	G13D	1.27	G13D	0.63
17	472	G13D	G13D	2.46	G13D	2.92
22	8	G12V	G12C	17.14	G12C	14.52
23	755	G13D	G13D	37.20	G13D	37.25
25	32	G12S	G12S	5.41	G12S	7.49

Digital PCR: clinical application 2

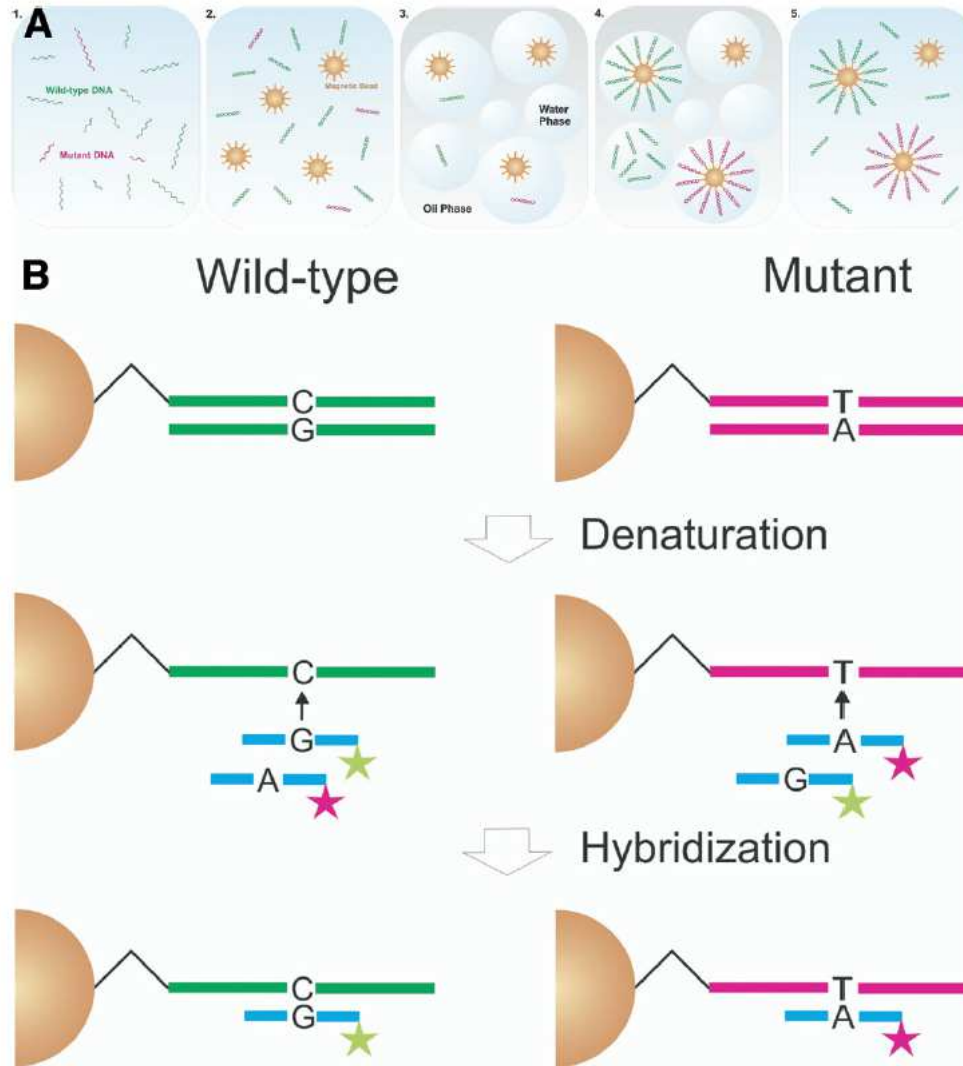
Analysis of Mutations in DNA Isolated From Plasma and Stool of Colorectal Cancer Patients

FRANK DIEHL,* KERSTIN SCHMIDT,* KRISTINE H. DURKEE,‡ KENT J. MOORE,‡ STEVE N. GOODMAN,§ ANTHONY P. SHUBER,|| KENNETH W. KINZLER,* and BERT VOGELSTEIN*

Background & Aims: Somatic mutations provide uniquely specific markers for the early detection of neoplasia that can be detected in DNA purified from plasma or stool of patients with colorectal cancer. The primary purpose of the present investigation was to determine the parameters that were critical for detecting mutations using a quantitative assay. A secondary purpose was to compare the results of plasma and stool DNA testing using the same technology. ***Methods:*** We examined DNA purified from the stool of 25 patients with colorectal cancers before surgery. In 16 of these cases, plasma samples also were available. Mutations in stool or plasma were assessed with an improved version of the BEAMing technology.

Results: Of the 25 stool DNA samples analyzed, 23 (92%) contained mutations that were present in the corresponding tumors from the same patients. In contrast, only 8 of the 16 (50%) plasma DNA samples analyzed had detectable levels of mutated DNA. We found that the DNA fragments containing mutations in both stool and plasma DNA typically were smaller than 150 bases in size. The sensitivity of the new method was superior to a widely used technique for detecting mutations, using single base extension and sequencing, when assessed on the same samples (92% vs 60%; $P = .008$, exact McNemar test). ***Conclusions:*** When assessed with sufficiently sensitive methods, mutant DNA fragments are detectable in the stool of more than 90% of colorectal cancer patients. DNA purified from stool provides a better template for mutation testing than plasma.

Digital PCR: clinical application 2



Digital PCR: clinical application 2

Table 2. Mutations in Stool and Plasma DNA

Patient	Sex/age, y	Stage (TNM)	Histology ^a	Tumor			Stool DNA			Plasma DNA			
				Site	Size, mm	Gene	Mutation (codon)	Total DNA fragments per 362 mg stool	Mutant DNA, %	Score	Total DNA fragments per 2 mL plasma	Mutant DNA, %	Score
1	M/66	I (T1N0M0)	Mod	R	50	APC	C2626T (876)	50,600	4.0	+			
2	F/64	I (T2N0M0)	Mod	Sig	30	APC	G3964T (1322)	398,000	0.87	+	3676	0.000	-
						TP53	G818A (273)	302,000	0.20	+			
3	F/70	I (T2N0M0)	Mod	C	45	APC	4237-4240delATGG (1413)	1808	0.71	+	2397	1.88	+
4	F/67	I (T1N0Mx)	Well	Tr	40	APC	C4132T (1378)	8460	0.39	+	9317	0.013	+
5	M/69	I (T2N0M0)	Well	Rs	24	APC	4359delT (1453)	1,030,000	0.000	-	3365	0.000	-
						KRAS	G35X (12) ^b	1,030,000	0.000	-			
6	M/84	I (T2N0M0)	Mod	R	25	APC	C2626T (876)	252,000	0.32	+			
						APC	4465delT (1489)	252,000	0.78	+			
						TP53	C742T (248)	252,000	1.0	+			
7	F/58	I (T2N0Mx)	Well	Sig	12	APC	4297delC (1433)	13,840	1.0	+			
						PIK3CA	C3075T (1025)	8260	21	+			
8	M/80	II (T3N0Mx)	Well	Sig	25	APC	4497delA (1499)	7420	0.003	-			
						KRAS	G38A (12)	7420	0.21	+			
9	M/70	II (T3N0Mx)	Well	Sf	50	APC	C3980G (1327)	59,600	15.0	+	10,652	0.002	-
						TP53	G524A (175)	59,600	0.3	+			
10	F/58	II (T3N0M0)	Well	Tr	80	APC	4467 delA (1489)	113,800	1.17	+	4530	0.002	-
11	F/65	II (T3N0M0)	Well	C	50	APC	4661-4662insA (1554)	106,600	1.09	+			
12	F/75	II (T3N0M0)	Well	R	25	APC	G4135T (1379)	540,000	0.37	+	4650	0.42	+
13	M/80	II (T3N0Mx)	Well	As	65	APC	C2626T (876)	264,000	0.06	+			
						APC	4189-4190delGA (1397)	264,000	0.04	+			
14	M/66	II (T3N0M0)	Mod	R	45	APC	C4348T (1450)	15,740	0.2	+	3690	0.005	-
						PIK3CA	G1624A (542)	5340	0.3	+			
15	F/50	III (T4N1M0)	Mod	R	25	APC	C4285T (1429)	22,600	0.13	+	6422	0.062	+
						KRAS	G35A (12)	22,600	0.2	+			
16	M/64	III (T3N1M0)	Poor	Sig	30	TP53	G524A (175)	6920	0.006	-	7047	0.033	+
17	M/74	III (T3N2M0)	Well	R	30	APC	4126-4127insT (1376)	7140	0.059	+	2679	0.17	+
						KRAS	G38A (12)	7140	0.079	+			
						PIK3CA	G1624A (542)	7140	0.050	+			
18	M/57	III (T3N1M0)	Mod/poor	Sig	70	APC	3934delG (1312)	18,700	0.28	+			
						TP53	G733A (245)	17,460	1.3	+			
19	F/65	III (T3N2Mx)	Mod/poor	As	50	APC	C2626T (876)	5920	0.18	+	11,716	0.002	-
						KRAS	G35C (12)	3320	0.23	+			
						TP53	C817T (273)	3320	0.10	+			
20	M/59	III (T3N1Mx)	Well	Tr	40	APC	4661-4662insA (1554)	11,320	0.0062	+			
						KRAS	G35A (12)	11,320	0.3	+			
21	M/73	III (T2N1Mx)	Mod	Tr	42	APC	C4348T (1450)	10,280	0.055	+	5043	0.007	-
						KRAS	G35A (12)	7200	0.23	+			
22	F/61	III (T3N1M0)	Mod	R	NR	APC	3980-3983delCAC (1327)	62,800	7.60	+	4206	0.001	-
						KRAS	G35A (12)	62,800	4.43	+			
23	M/67	IV (T3N2M1)	Mod	Sig	60	PIK3CA	C1636A (546)	138,000	0.068	+	29,233	6.6	+
24	M/65	IV (T3N1M1)	Well	As	30	APC	G4189T (1397)	254,000	0.62	+	4094	0.44	+
						PIK3CA	A3140G (1047)	254,000	1.33	+			
25	M/64	NR	NR	R	35	APC	3927-3931del AAAGA (1309)	356,000	0.90	+			
						TP53	G524A (175)	356,000	10.2	+			

Digital PCR: clinical application 3

Single-Molecule Detection of Epidermal Growth Factor Receptor Mutations in Plasma by Microfluidics Digital PCR in Non – Small Cell Lung Cancer Patients

Tony K.F. Yung,^{1,2} K.C. Allen Chan,^{1,2} Tony S.K. Mok,^{1,3} Joanna Tong,⁴ Ka-Fai To,⁴ and Y.M. Dennis Lo^{1,2,5}

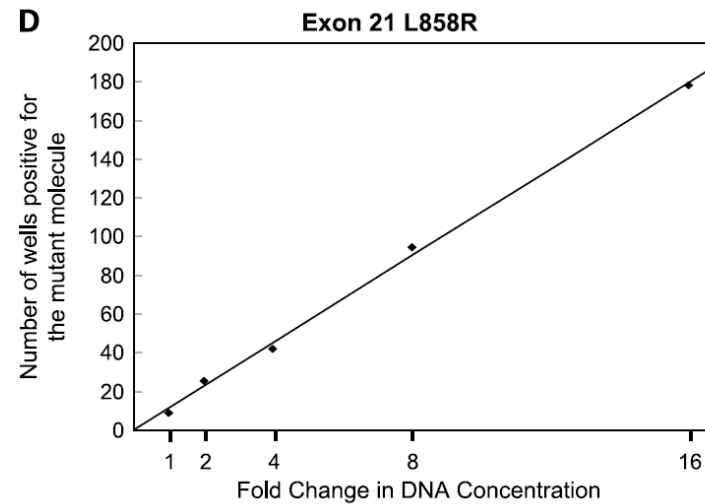
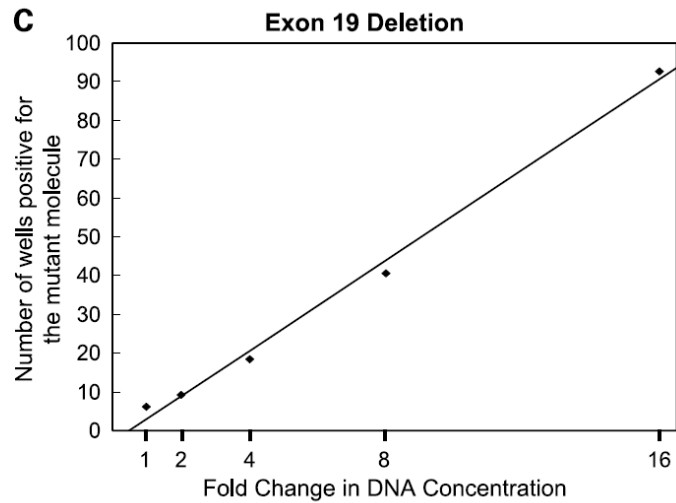
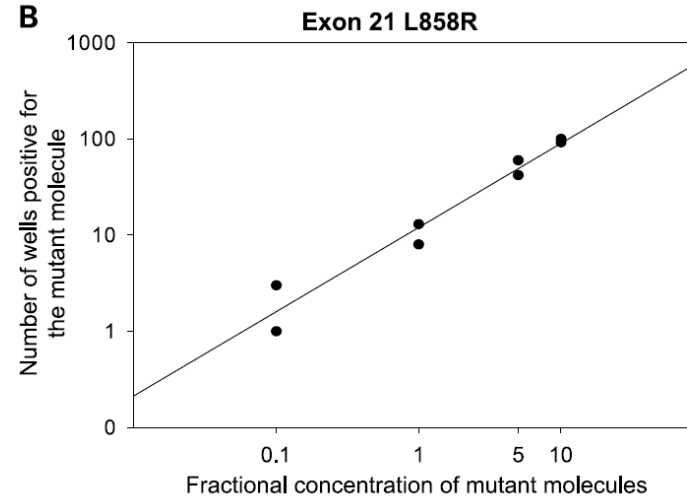
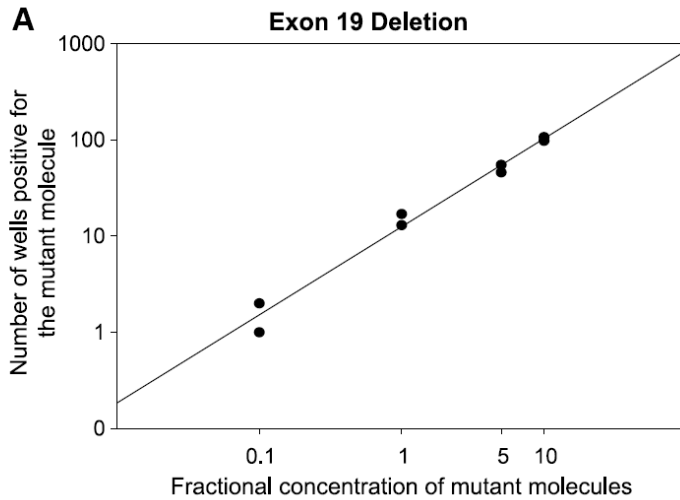
Abstract **Purpose:** We aim to develop a digital PCR-based method for the quantitative detection of the two common epidermal growth factor receptor (*EGFR*) mutations (in-frame deletion at exon 19 and L858R at exon 21) in the plasma and tumor tissues of patients suffering from non-small cell lung cancers. These two mutations account for >85% of clinically important *EGFR* mutations associated with responsiveness to tyrosine kinase inhibitors.

Experimental Design: DNA samples were analyzed using a microfluidics system that simultaneously performed 9,180 PCRs at nanoliter scale. A single-mutant DNA molecule in a clinical specimen could be detected and the quantities of mutant and wild-type sequences were precisely determined.

Results: Exon 19 deletion and L858R mutation were detectable in 6 (17%) and 9 (26%) of 35 pretreatment plasma samples, respectively. When compared with the sequencing results of the tumor samples, the sensitivity and specificity of plasma *EGFR* mutation analysis were 92% and 100%, respectively. The plasma concentration of the mutant sequences correlated well with the clinical response. Decreased concentration was observed in all patients with partial or complete clinical remission, whereas persistence of mutation was observed in a patient with cancer progression. In one patient, tyrosine kinase inhibitor was stopped after an initial response and the tumor-associated *EGFR* mutation reemerged 4 weeks after stopping treatment.

Conclusion: The sensitive detection and accurate quantification of low abundance *EGFR* mutations in tumor tissues and plasma by microfluidics digital PCR would be useful for predicting treatment response, monitoring disease progression and early detection of treatment failure associated with acquired drug resistance.

Digital PCR: clinical application 3



Digital PCR: clinical application 3

Table 2. Digital PCR detection of *EGFR* mutations in plasma collected before treatment

Patient	Tumor tissue		Plasma		Response to TKI treatment if treated with TKI*	
	CSGE and sequencing analysis ^{† ‡}	Digital PCR analysis [§]		Digital PCR analysis [§]		
		Del19 mutant percentage	L858R mutant percentage	Mutation		Concentration (copies/mL)
(A) Mutations detected by digital PCR and by CSGE and sequencing						
Case 8	L858R	ND	40	L858R	3.2	PR
Case 15	L858R	ND	19	L858R	55	PD
Case 20	L858R	ND	23	L858R	3.2	—
Case 29	L858R	ND	87	L858R	29	—
Case 38	L858R	ND	39	L858R	34,000	CR
Case 39	L858R	ND	26	L858R	9.7	PR
Case 37	L858R	ND	5.2	None	ND	—
Case 11	Del19	65	ND	Del19	21	PR
Case 13	Del19	42	ND	Del19	140	—
Case 17	Del19	38	ND	Del19	890	—
Case 31	Del19	68	ND	Del19	200	—
Case 40	Del19	32	ND	Del19	49	—
(B) Mutations detected by digital PCR (CSGE and sequencing was unsuccessful)						
Case 18	Failed	56	3.9	Del19	22	—
Case 26	Failed	ND	62	L858R	8,300	PR
Case 30	Failed	ND	64	L858R	52	—
Case 34	Failed	ND	45	L858R	500	—
(B) Mutations detected by digital PCR but not by CSGE and sequencing						
Case 3	Wild-type only	ND	3.4	None	ND	—
Case 4	Wild-type only	ND	2.0	None	ND	—
Case 19	Wild-type only	4.6	ND	None	ND	—
(C) No mutation detected in tumor						
Case 5	Wild-type only	ND	ND	None	ND	—
Case 6	Wild-type only	ND	ND	None	ND	—
Case 10	Wild-type only	ND	ND	None	ND	—

Digital PCR: Patents

WO 2013/113816

PCT/EP2013/051899

-23-

Determination of TP53 as exemplary tumor marker

For detection of tumor cells the fact that already very early in the progression of ovarian cancer in most of the patients, a mutation of the TP53 gene is likely to occur is used. The mutation is detected for example through digital PCR, using the QX100™ Droplet Digital™ PCR System from Bio-RAD. The type of TP53 mutation present in the primary tumor tissue is verified in the DNA isolated from the lavage. Therefore, an assay targeting this specific TP53 mutation is designed. It uses a forward and a reversed primer, which bind upstream and downstream the targeted region. A PCR product of ~100bp is produced. Probes which are specific for the particular TP53 mutation, respectively wild type are used. These probes must have a melting temperature T_m 5-10°C higher than the primer T_m . The probes consist of a fluorophore covalently attached to the 5'-end, for the mutation specific probe FAM (6-carboxyfluorescein), for the wild type VIC and a quencher on the 3'-end MGB (minor groove binder). The PCR components (Master mix, primers, probes, DNA) are mixed and 20 µl of this mix are used for droplet generation using the QX100™ Droplet Generator from Bio-RAD, according to manufacturer's protocol. By that the PCR Assay is partitioned into 20,000 water in oil droplets. The emulsion is then transferred to a 96-well PCR plate, heat sealed and PCR is performed. Annealing temperature is adapted to previous optimized temperature, depending on which kind of TP53 mutation is going to be detected. Through the QX100™ Droplet Reader (Bio-RAD) each droplet is counted as negative or positive for the specific target DNA and if a cell carrying a TP53 mutation was present in the lavage, a fluorescent signal is detected.

The TP53 gene expression, specifically the mutation and overexpression of p53, is indicative of a disease, specifically OC and/or EC, or a precursor malignancy thereof.

According to the example, the following p53 mutation is determined employing the primer and probes described herein:

30 Mutation in codon 248 (g.14070G>A, p.Arg248Gln)

forward PCR primer: tgtaacagttcctgcatgggc (SEQ ID 1)

reverse PCR Primer: acagcaggccagtggtgca (SEQ ID 2)

WO 2013/113816

PCT/EP2013/051899

-24-

probe 1: 5'-FAM-catgaaccagaggcc-MGB-3' (SEQ ID 3)

probe 2: 5'-VIC-catgaaccggaggcc-MGB-3' (SEQ ID 4)

TP53 gene: UniProtKB: P04637

5 This gene encodes tumor protein p53, which acts as a tumor suppressor in many tumor types; induces growth arrest or apoptosis depending on the physiological circumstances and cell type. Involved in cell cycle regulation as a trans-activator that acts to negatively regulate cell division by controlling a set of genes required for this process. One of the activated genes is an inhibitor of cyclin-dependent kinases.

10 Apoptosis induction seems to be mediated either by stimulation of BAX and FAS antigen expression, or by repression of Bcl-2 expression. Implicated in Notch signaling cross-over. Prevents CDK7 kinase activity when associated to CAK complex in response to DNA damage, thus stopping cell cycle progression. Isoform 2 enhances the transactivation activity of isoform 1 from some but not all TP53-inducible

15 promoters. Isoform 4 suppresses transactivation activity and impairs growth suppression mediated by isoform 1. Isoform 7 inhibits isoform 1-mediated apoptosis.

Alternatively a method of targeted deep sequencing of genetic alterations may be used, e.g. those known to occur in ovarian and endometrial and tubal cancer frequently.

COLD-PCR and Digital PCR

- COLD-PCR is enrichment technique; digital PCR is for detection.
- They can be used in tandem for maximal sensitivity.
- Pre-amplification may impair accuracy for quantification by digital PCR.

COLD-PCR and digital PCR

	COLD-PCR	Digital PCR
Run time	2 – 7 h	1 – 3 h
Cost	~ \$3 per sample	\$3 per sample (BioRad)
Throughput	96 well plate	8 samples / chip
Sensitivity (mutant/wt ratio)	0.1% (~100 fold enrichment)	10^{-6}
Multiplexity	Up to 10 different alleles using HRMA for detection.	Up to 5 different alleles.
Advantage	- Can enrich unknown mutation.	- No need of external detection. - Works equally well with all types of mutations.
Disadvantage	- Need to fine-tune Tc. - Works better for certain mutations than others. - May need off-line detection. - No quantification.	- Must know the mutation.

Detection of *IDH1* mutation in the plasma of patients with glioma

ABSTRACT

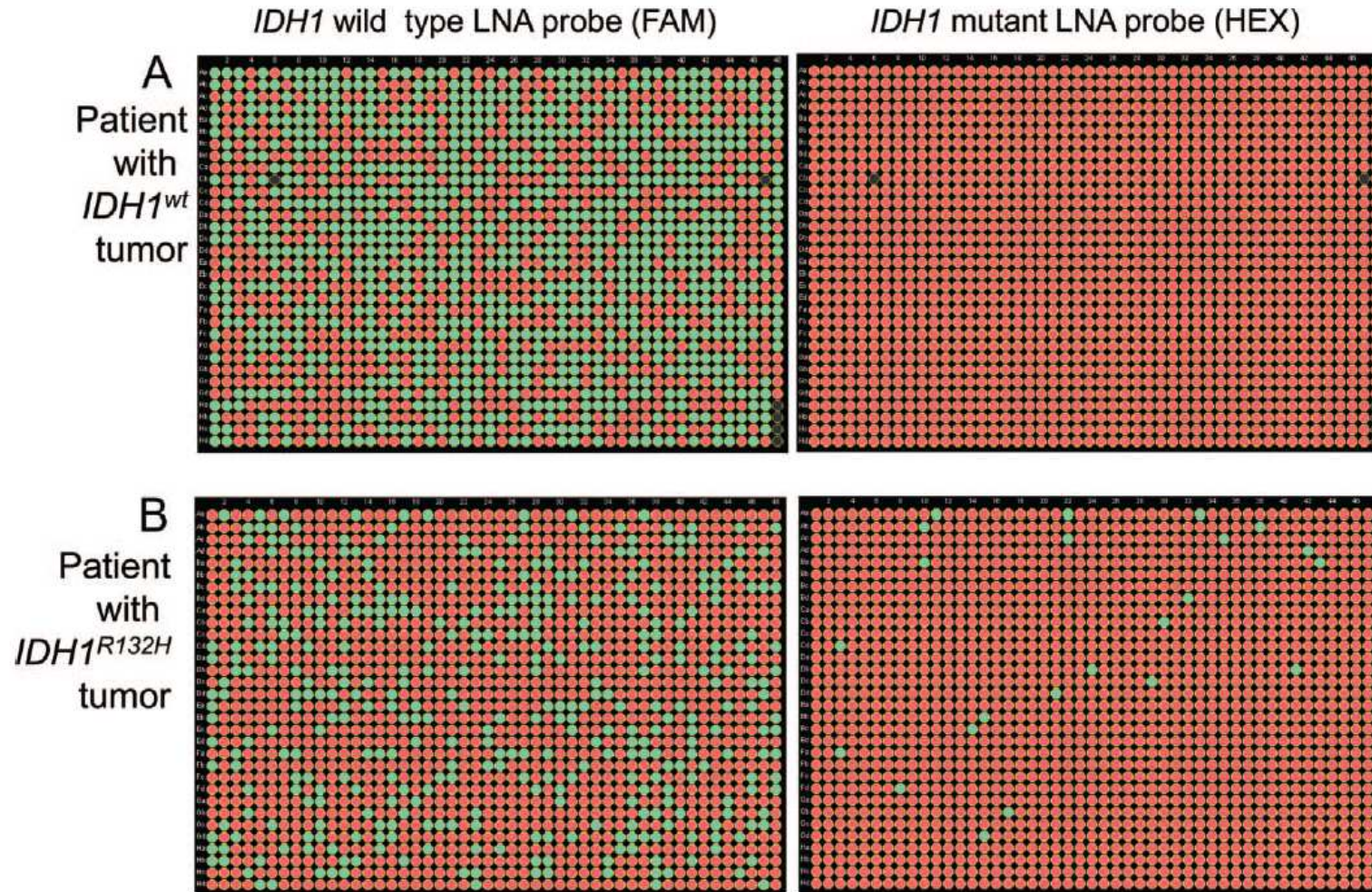
Objective: The *IDH1*^{R132H} mutation is both a strong prognostic predictor and a diagnostic hallmark of gliomas and therefore has major clinical relevance. Here, we developed a new technique to detect the *IDH1*^{R132H} mutation in the plasma of patients with glioma.

Methods: Small-size DNA (150–250 base pairs) was extracted from the plasma of 31 controls and 80 patients with glioma with known *IDH1*^{R132H} status and correlated with MRI data. The *IDH1*^{R132H} mutation was detected by a combination of coamplification at lower denaturation temperature and digital PCR.

Results: The small size DNA concentration was 1.2 ng/mL (range 0.1–6.6) in controls vs 1.2 ng/mL (range 0.1–50.3) in patients with glioma ($p =$ not significant) and 0.9 ng/mL (0.0–3.0) in low-grade gliomas vs 1.5 ng/mL in high-grade gliomas ($p < 0.01$). The small size DNA concentration correlated with enhancing tumor volume (1.6 ng/mL [0.4–24.9] when $<10 \text{ cm}^3$ and 14.0 ng/mL [0.6–50.3] when $\geq 10 \text{ cm}^3$). The *IDH1*^{R132H} mutation was detected in 15 out of 25 plasma DNA mixtures (60%) from patients with mutated tumors and in none of the 14 patients with a nonmutated tumor. The sensitivity increased with enhancing tumor volume (3/9 in nonenhancing tumors, 6/10 for enhancing volume $<10 \text{ cm}^3$, and 6/6 for enhancing volume $\geq 10 \text{ cm}^3$).

Conclusion: With a specificity of 100% and a sensitivity related to the tumor volume and contrast enhancement, *IDH1*^{R132H} identification has a valuable diagnostic accuracy in patients not amenable to biopsy. **Neurology**® 2012;79:1693–1698

COLD-PCR and digital PCR



COLD-PCR and digital PCR

Table 3 *IDH1* mutation detection in the plasma according to grade and tumor volume^a

	FLAIR (A, B, C) or T1 postcontrast (D, E, F) volume	No.	<i>IDH1</i> ^{wt} patients	<i>IDH1</i> ^{R132H} patients, n (%)
Low-grade gliomas				
All		12	0/4	3/8 (37.5)
Group A	<2.5 cm ³	—	—	—
Group B	2.5 cm ³ < V < 22.5 cm ³	3	0/1	0/2 (0)
Group C	>22.5 cm ³	9	0/3	3/6 (50)
High-grade gliomas				
All		27	0/10	12/17 (70.6)
Group D	0 cm ³	1	0/0	0/1 (0)
Group E	0 cm ³ < V < 10 cm ³	14	0/4	6/10 (60)
Group F	>10 cm ³	12	0/6	6/6 (100)

Abbreviation: FLAIR = fluid-attenuated inversion recovery.

^a *IDH1*^{R132H} mutation detection efficiency is more dependent on the volume of the enhancing tumors (groups D, E, and F) than that of the nonenhancing tumors (groups A, B, and C).

What can we do?

- Enhancing reagent for COLD-PCR (HRMA or HPLC).
- Enhancing reagent for Digital PCR.
 - Would the organic solvent disturb the water-in-oil droplets?
- Tandem COLD-PCR with digital PCR.
- Multiplex detection.
- Optimal control.

Optimal Control of DNA Amplification: noncompetitive problems

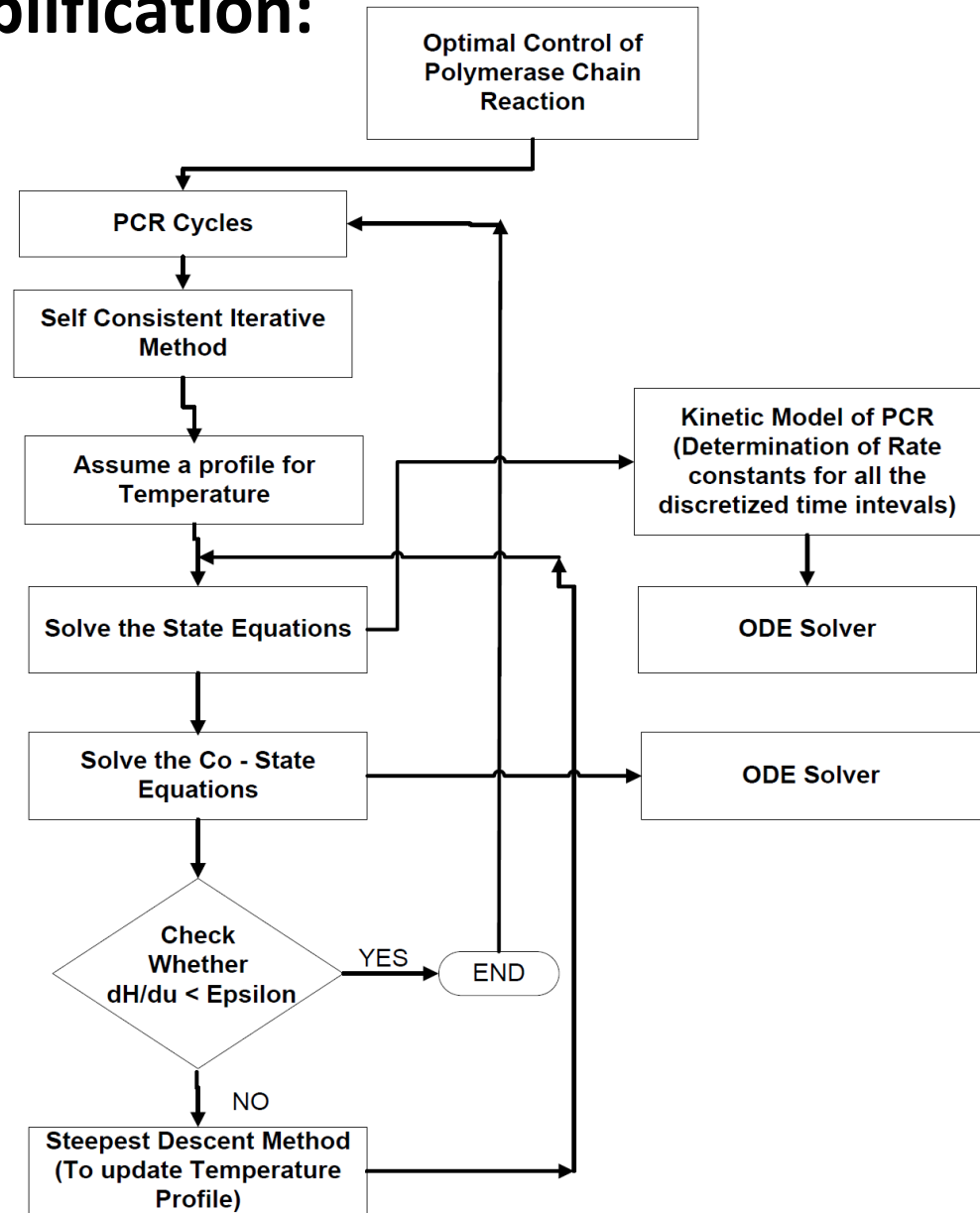
$$\text{Min}_{T(t)} \left(C_{DNA}(t_f) - C_{DNA}^{\max} \right)^2$$

$$\text{st } \frac{dx}{dt} = f(x, T)$$

$$x = \left[C_{S_1}, C_{S_2}, \dots, C_{E.D_1}, \dots, C_{DNA} \right]^{Tr}$$

For N nucleotide template –
2N + 4 state equations

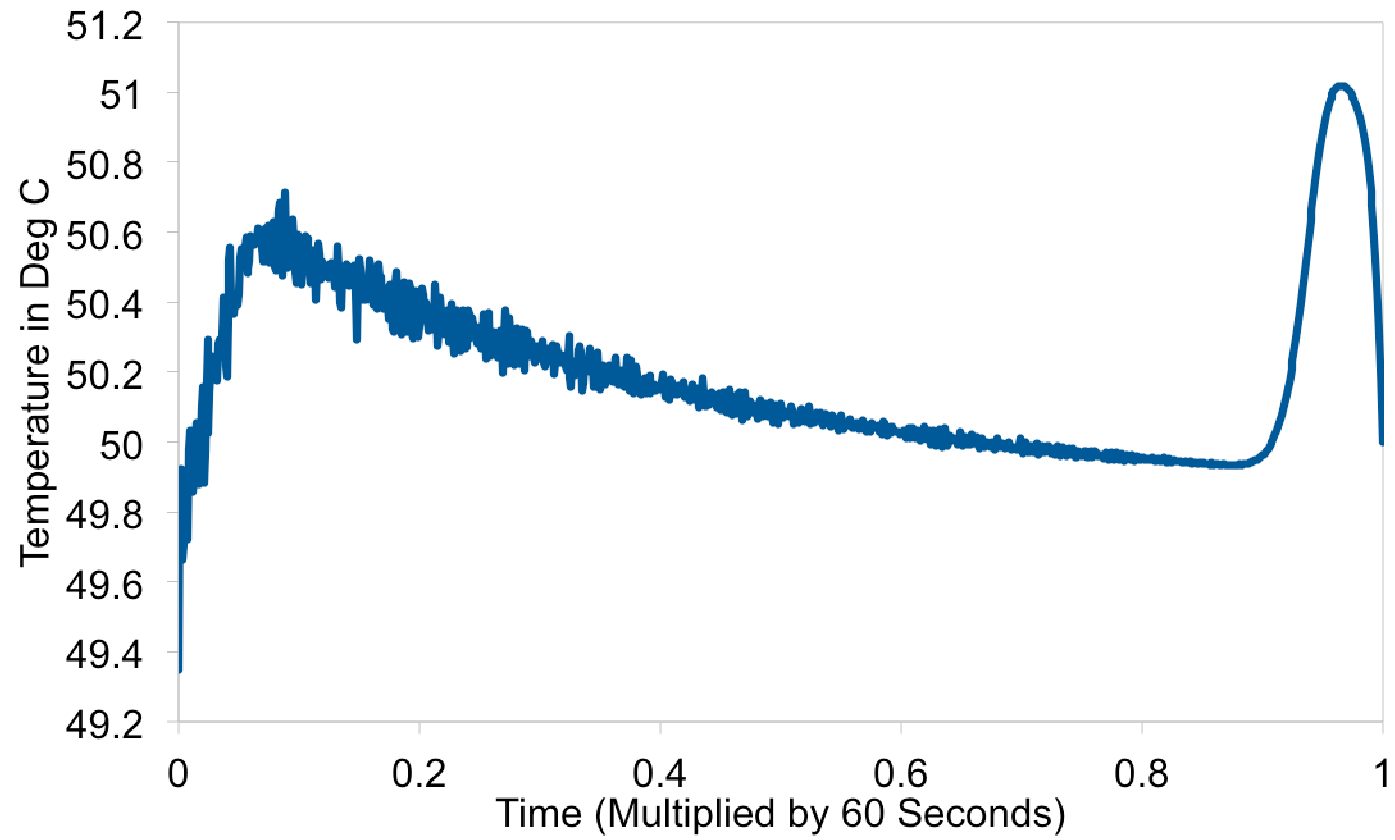
Typically N ~ 10³



R. Chakrabarti et al. Optimal Control of Evolutionary Dynamics, *Phys. Rev. Lett.*, 2008

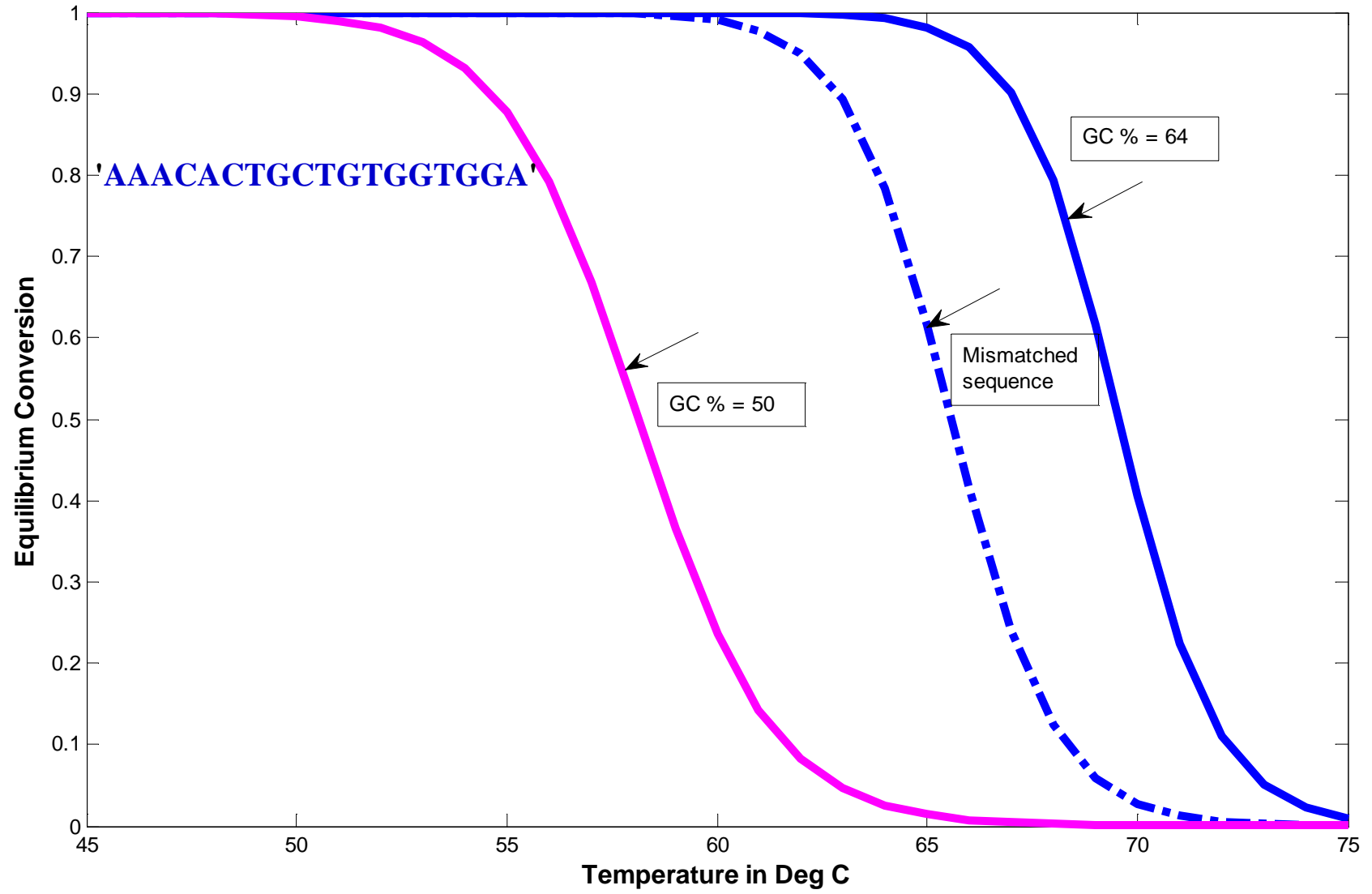
K. Marimuthu and R. Chakrabarti, Optimally Controlled DNA amplification, in preparation

Preliminary Results of the OCT



Competitive hybridization of mismatched primers

'CTC**G**AGGTCCAGAGTACCCGCTGTG'
'GAG**G**TCCAGGTCTCATGGGCGACAC'



Optimal Control of DNA Amplification: competitive problems

- Optimal control: critical to determine annealing/extension profile. Maximize target species, minimize nonspecific hybrids.
- Requires controllability over higher dimensional subspace than noncompetitive problems

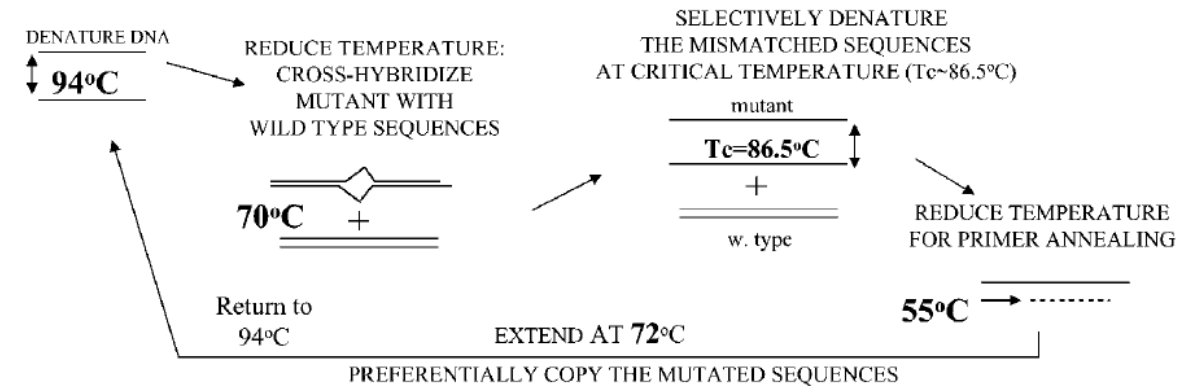
$$\text{Min}_{T(t)} \quad w_1 \left(C_{DNA}(t_f) - C_{DNA}^{\max} \right)^2 - w_2 \left(C_{DNA}^{non\ specific}(t_f) \right)^2$$

$$\text{st} \quad \frac{dx}{dt} = f(x, T)$$

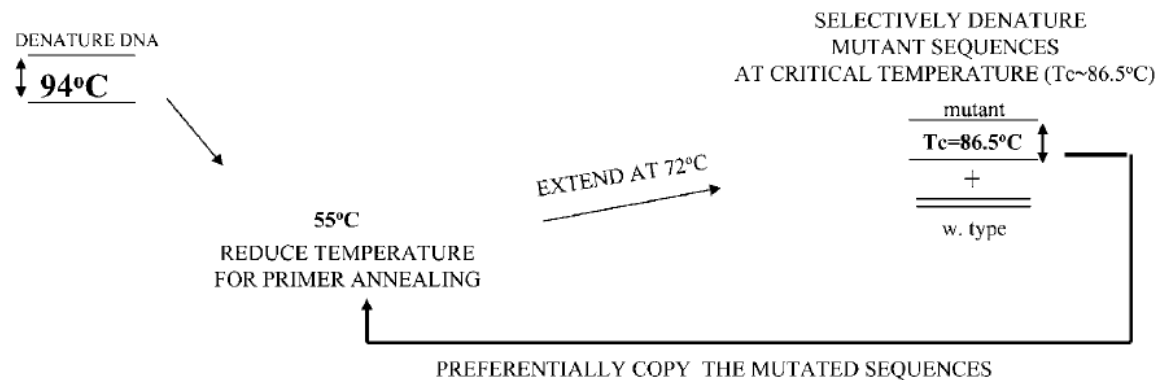
$$x = \left[C_{s_1}, C_{s_2}, \dots, C_{E.D_1} \dots C_{DNA}, C_{s_1}^{ns}, C_{s_2}^{ns}, \dots, C_{E.D_1}^{ns} \dots C_{DNA}^{ns} \right]$$

Competitive amplification example 2: mutation enrichment

A. FULL COLD-PCR (FOR ENRICHMENT OF ALL MUTATIONS)



B. FAST COLD-PCR (FOR ENRICHMENT OF T_m-REDUCING MUTATIONS)



▪ Mutation Enrichment:

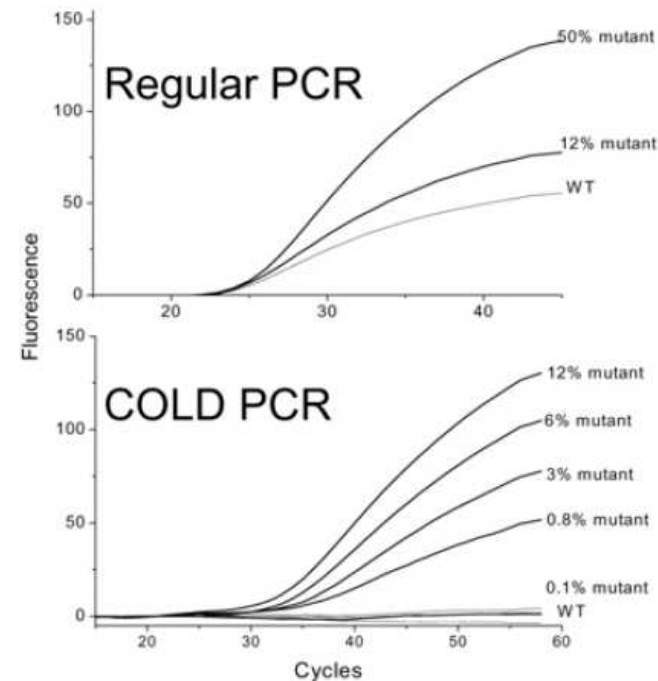
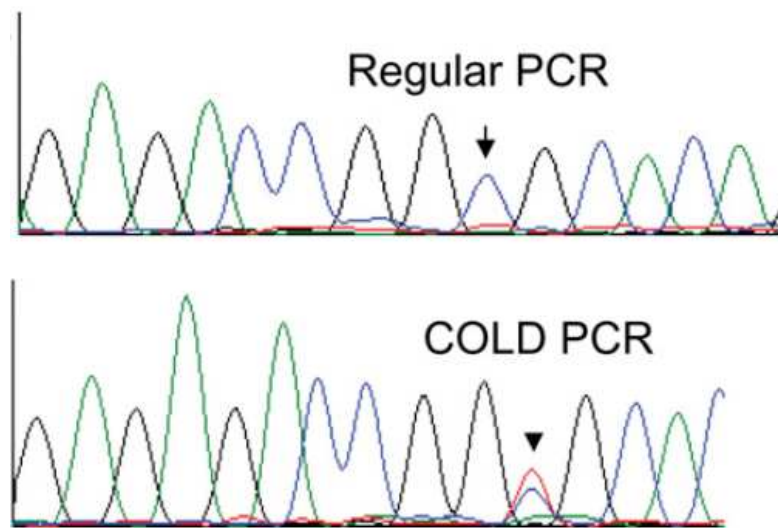
competition between mutant DNA causing cancer and wild-type DNA amplification.

▪ A competitive amplification problem in diagnostics that has been addressed w/ only equilibrium cycling strategies

▪ State-of-the-art approach: **COLD PCR** (licensed by Transgenomic from HMS)

Competitive amplification example 2: COLD PCR mutation enrichment

- For: metastasis (blood, primarily detection); diagnosis (tumor cells)
- K-ras, p53 are tumor suppressors: mutations strongly correlated w prognosis
- COLD PCR reduces detection limit from 10% to 0.1-1%



- **COLD PCR** deals with the competition by introducing an additional step (heteroduplex hybridization). Slows down the PCR procedure.
- **Optimally controlled PCR**: for fixed time per cycle, solve the problem of **maximizing single stranded mutant DNA concentration while minimizing double stranded wild-type concentration**, through kinetic modeling and OCT.

Outline

- Background: cancer biomarker in blood plasma
- COLD-PCR
 - How it works
 - Different protocols
 - Detection technologies
 - Clinical applications
- Digital PCR
 - How it works
 - Comparison with qPCR
 - Instrumentation
 - Clinical applications
- COLD-PCR and digital PCR
- **Detection of tri- and hexa-nucleotide repeat expansion**

Trinucleotide repeats in Human Genetic Diseases

Table 1 Trinucleotide repeat expansions in humans

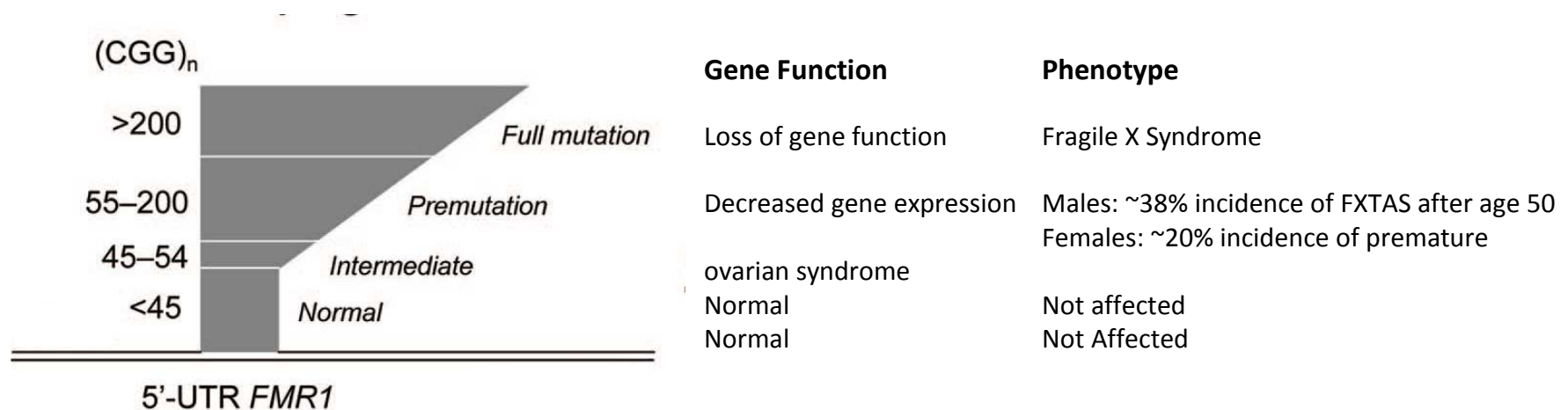
Locus	Disorder	Repeat Alleles		Repeat location	Functional consequence of expansion
		Normal	Mutant		
<i>FMRI</i> (<i>FRAXA</i>)	Fragile X syndrome	(CGG) ₆₋₅₂	(CGG) ₆₀₋₂₀₀ (premutation) (CGG) ₂₃₀₋₁₀₀₀ (full)	5'-UTR	Loss-of-function Fragile site
<i>FRAXE</i>	Fragile XE mental retardation	(GCC) ₇₋₃₅	(GCC) ₁₃₀₋₁₅₀ (premutation) (GCC) ₂₃₀₋₇₅₀ (full)	ND ^a	Fragile site Loss-of-function ?
<i>FRAXF</i>	None	(GCC) ₆₋₂₉	(GCC) ₃₀₀₋₁₀₀₀	ND	Fragile site
<i>FRA16A</i>	None	(CCG) ₁₆₋₄₉	(CCG) ₁₀₀₀₋₁₉₀₀	ND	Fragile site
<i>FRA11B</i> (<i>CBL2</i>)	Predisposition toward Jacobsen (11q-) syndrome in offspring	(CGG) ₁₁	(CGG) ₈₀ (premutation) (CGG) ₁₀₀₋₁₀₀₀ (full)	5'UTR	Fragile site
<i>AR</i>	Spinal and bulbar muscular atrophy	(CAG) ₁₁₋₃₃	(CAG) ₃₈₋₆₆	Coding	Gain and partial loss-of-function
<i>SCA1</i>	Spinocerebellar ataxia Type 1	(CAG) ₆₋₃₉	(CAG) ₄₁₋₈₁	Coding	Gain of function
<i>Hdh</i> (<i>IT15</i>)	Huntington's disease	(CAG) ₁₀₋₃₅	(CAG) ₃₆₋₁₂₁	Coding	Gain of function
<i>B37</i> (<i>DRPLA</i>)	Dentatoribral-pallidoluyisian atrophy Haw River syndrome (phenotypic variant)	(CAG) ₇₋₂₅	(CAG) ₄₉₋₇₅ (CAG) ₆₃₋₆₈	Coding	Gain of function
<i>MJD1</i> (<i>SCA3</i>)	Machado-Joseph disease	(CAG) ₁₂₋₃₇	(CAG) ₆₁₋₈₄	Coding	Gain of function
<i>DMPK</i>	Myotonic dystrophy	(CTG) ₅₋₃₇	(CTG) ₅₀₋₃₀₀₀	3'UTR	Processing of <i>DMPK</i> Message abnormal?

^aND = not determined

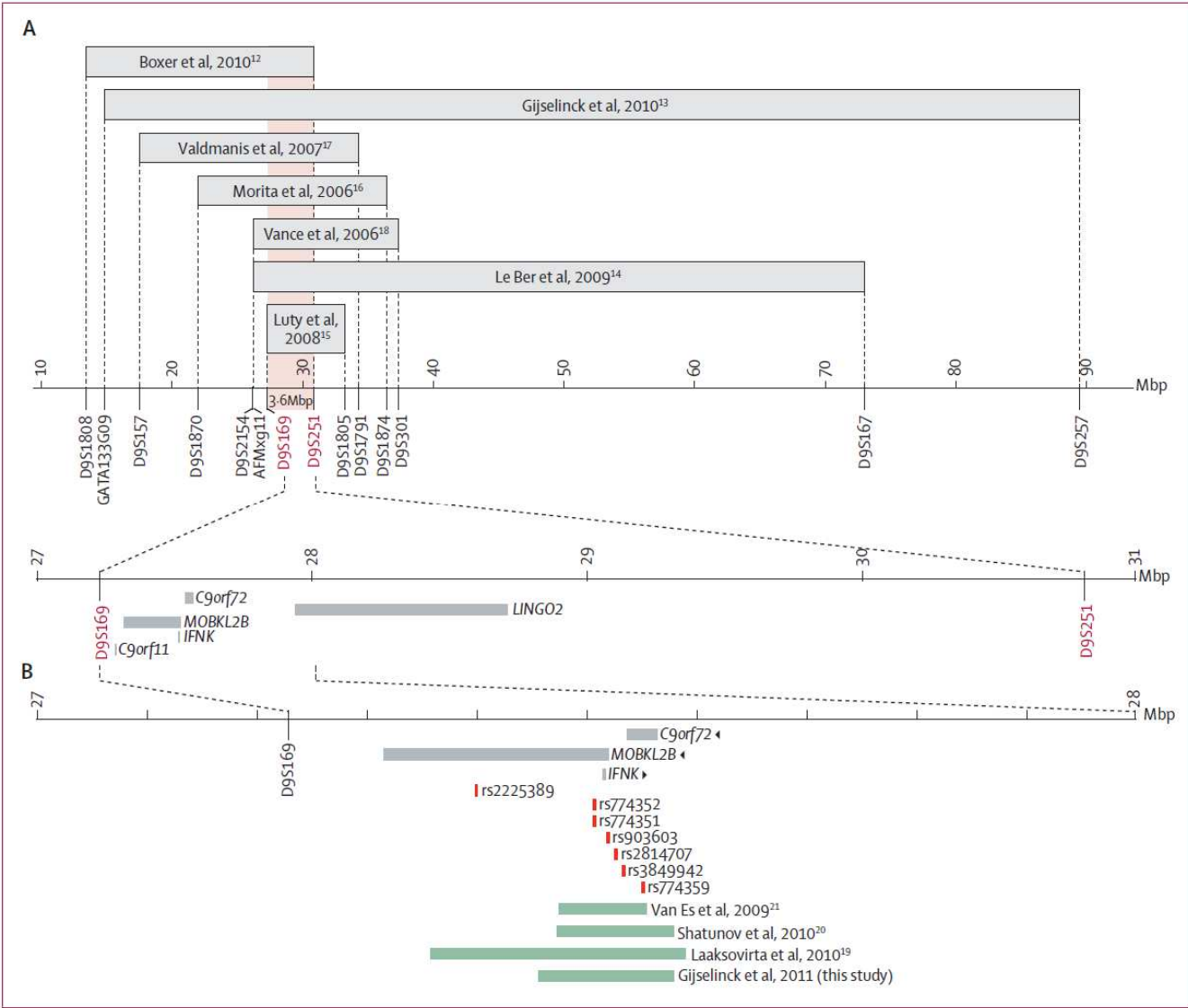
Fragile X syndrome and (CGG) triplet expansion

Expansion of the CGG

repeats results in methylation of the promoter region, which silences the expression of the FMR1 protein (FMRP). FMRP normally binds to and facilitates the translation of a number of essential RNAs that are present in neurons. In FRAX, neuronal RNAs for FMR1 are not translated into protein leading to abnormal neural development via undefined mechanisms.



Neurodegenerative disease FTLD/ALS



C9orf72 (GGGGCC) expansion

	FTLD (n=337)	FTLD-ALS (n=23)	ALS (n=141)	Controls (n=859)
Age (years)*	62.9 (9.7)	62.6 (10.0)	59.9 (11.6)	65.3 (14.8)
Sex (male)	188 (56%)	10 (43%)	85 (60%)	357 (42%)
Positive family history	101 (30%)	7 (30%)	16 (11%)	..
Autopsy diagnosis	21 (6%)	3 (13%)	5 (4%)	..
FTLD-associated genes				
<i>GRN</i>	24 (7%)	0	NA	0
→ <i>C9orf72</i>	21 (6%)	7 (30%)	13 (9%)	0
<i>MAPT</i>	4 (1%)	0	NA	NA
<i>VCP</i>	2 (1%)	0	0	NA
<i>CHMP2B</i>	1 (<1%)	0	NA	NA
<i>PSEN1</i>	1 (<1%)	0	NA	NA
ALS-associated genes				
→ <i>C9orf72</i>	21 (6%)	7 (30%)	13 (9%)	0
<i>SOD1</i>	NA	0	0	NA
<i>TARDBP</i>	NA	0	1 (1%)	NA
<i>FUS</i>	NA	0	1 (1%)	NA
<i>ATXN2</i>	NA	0	2 (1%)	NA
Total mutations	53 (16%)	7 (30%)	17 (12%)	NA

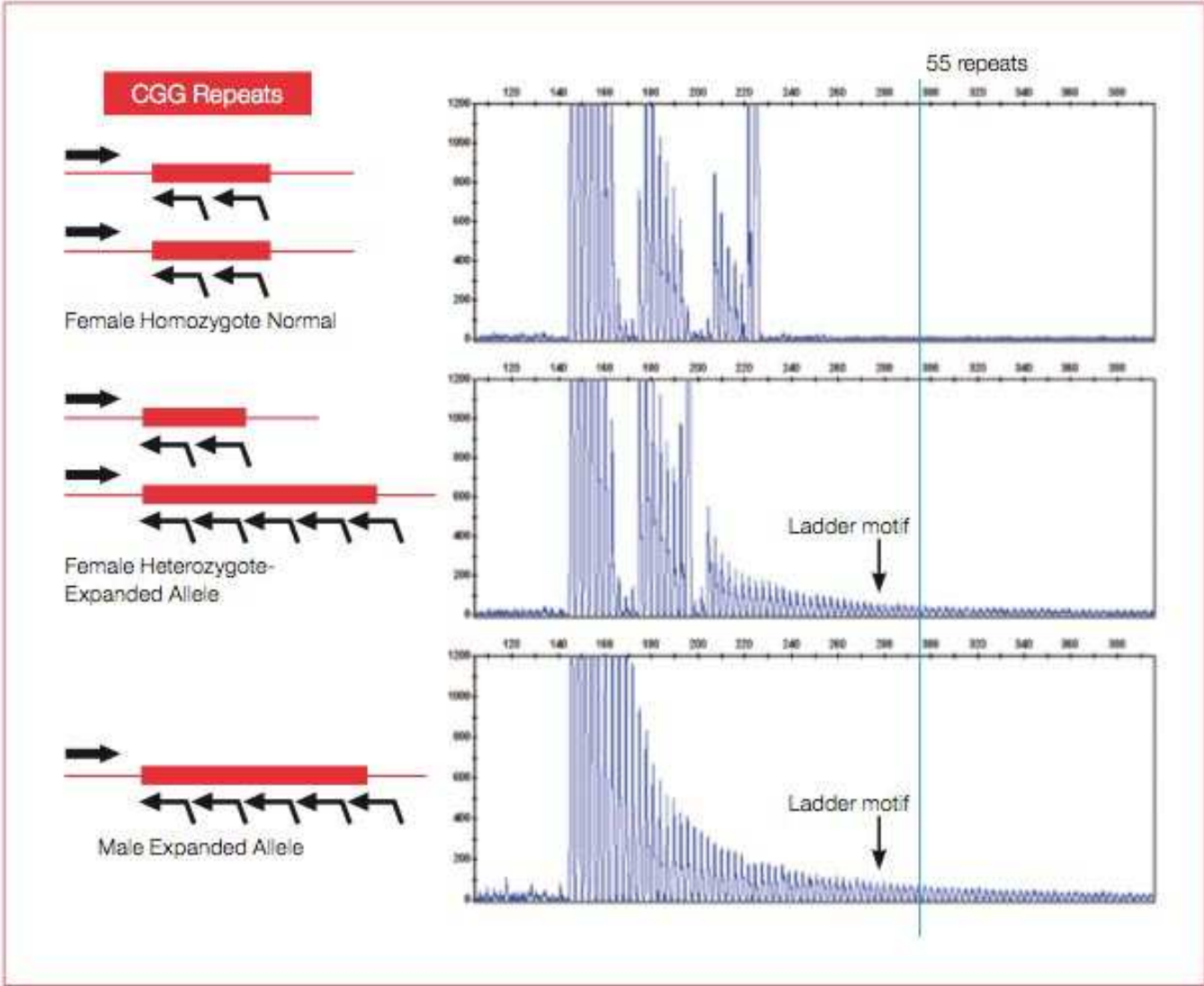
Data are mean (SD) or n (%). ALS=amyotrophic lateral sclerosis. FTLD=frontotemporal lobar degeneration. ..=not applicable. NA=not assessed. *Age at onset or age at inclusion (for controls).

Table 1: Demographic and genetic characteristics of the Flanders-Belgian cohort

C9orf72 (GGGGCC) expansion

- In the normal population, non-expanded C9orf72 repeat sizes range from 2 to 24 G₄C₂ units.
- The size distribution of pathologically expanded alleles is not well defined, but generally exceeds 60 repeat units, the detection limit of the commonly used repeat-primed PCR technology. Southern blot hybridization experiments in a limited number of repeat expansion carriers suggested somatically instable sizes of 700 to 4400 units.
- Apart from rarely observed alleles between 24 and 60 repeat units, a significant size gap seems to exist, which might suggest that repeats larger than 24 units are prone to rapid further expansion.
- The C9orf72 gene is transcribed as three major messengers (transcript variants 1 to 3) encoding two protein isoforms (C9orf72a and b).
- C9orf72 is widely conserved in the animal kingdom but none of the orthologous genes have a known function.

Detection Methods: repeat-primed PCR



Detection Methods: repeat-primed PCR

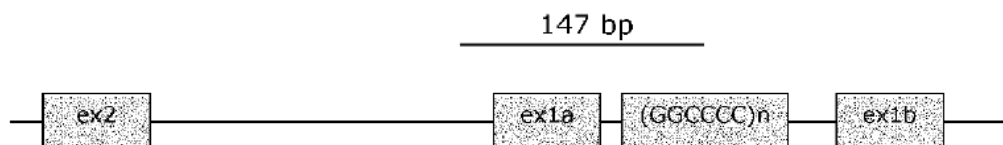
(10) International Publication Number
WO 2013/041577 A1

Applicants: VIB VZW [BE/BE]; Rijvisschestraat 120, B-9052 Gent (BE). UNIVERSITEIT ANTWERPEN [BE/BE]; Prinsstraat 12, B-2000 Antwerpen (BE).

Inventors: VAN BROECKHOVEN, Christine; Koning Albertlei 15, B-2650 Edegem (BE). CRUTS, Marc; Belegstraat 73, B-2018 Antwerpen (BE).

(54) Title: METHODS FOR THE DIAGNOSIS OF AMYOTROPHIC LATERAL SCLEROSIS AND FRONTOTEMPORAL LOBAR DEGENERATION

Figure 1



(57) **Abstract:** The invention relates to the detection of mutations in the promoter region of the gene C9ORF72, in particular a hexanucleotide expansion, wherein said mutations cause a significant decrease in the expression of gene C9ORF72. The decrease in gene C9ORF72 expression is related to the presence of amyotrophic lateral sclerosis (ALS) or frontotemporal lobar degeneration (FTLD), and the mutations can be used in the diagnosis of ALS and/or FTLD, or in the construction of transgenic animals for studying ALS and/or FTLD.

Detection Methods: repeat-primed PCR

PCR Primers:

F: 5'-TCCTCACTCACCCACTCG-3'

R1: 5'-CGTACGCATCCCAGTTTGAGAGGGGGCCGGGGCCGGGGCCGGGGC-3'

R2: 5'-CGTACGCATCCCAGTTTGAGA-3'

PCR Protocol

DNA (100ng/μl)	1μl	<u>98°C</u> 10'
Buffer 2	2μl	97°C 35''
dNTP (10mM) 1μl		10 cycli - 53°C - 35''
F primer (10μM)	0.66μl	<u>68°C</u> 2'
R1 primer (10μM)	0.066μl	97°C 35''
R2 primer (10μM)	0.66μl	25 cycli 53°C 35''
Betaine (3M)	13.86μl	<u>68°C</u> 2' (+20'' for each successive) cycle)
Enzyme**	0.75μl	68°C 10'
		4°C forever

Detection methods: Sudha's work on FMR1

												Expected pdt size for 54rpt gDNA (NA20230)
I											mRNA start	
	13681	cagcgggccc	ggggttcggc	ctcagtcagg	cGCTCAGCTC	CGTTTCGGTT	TCACTTCCGG					
	13741	T ggagggccc	cctctgagcg	ggcggcgggc	cgacggcgag	cgcgggcggc	ggcggtgacg					
	13801	gaggcgccgc	tgccaggggg	cgtgcggcag	cg ggcggcg	gcggcggcg	cggcggcggc					
	13861	ggagggcggcg	gcggcggcg	cggcggcggc	gg ctgggcct	cgagcgcccg	cagcccacct					
	13921	ctcggggggcg	ggctcccggc	gctagcaggg	ctgaagagaa	ga TGGAGGAG	CTGGTGGTGG					
											protein start	
	13981	AAGTGCGGGG	CT ccaatggc	gctttctaca	aggtacttgg	ctctagggca	ggccccatct					
	14041	tcgcccttcc	ttccctccct	tttcttcttg	gtgtc							
II											mRNA start	
	13681	cagcgggccc	ggggttcggc	ctcag TCAGG	CGCTCAGCTC	CGTTTCGGTT	TCA cttccgg					
	13741	tggagggccc	cctctgagcg	ggcggcgggc	cgacggcgag	cgcgggcggc	ggcggtgacg					
	13801	gaggcgccgc	tgccaggggg	cgtgcggcag	cg ggcggcg	gcggcggcg	cggcggcggc					
	13861	ggagggcggcg	gcggcggcg	cggcggcggc	gg ctgggcct	cgagcgcccg	cagcccacct					
	13921	ctcggggggcg	ggctcccggc	gctagcaggg	ctgaagagaa	gat ggaggag	ctggtggt GG					
											protein start	
	13981	AAGTGCGGGG	CTCCAATGGC	GCTT tctaca	aggtacttgg	ctctagggca	ggccccatct					
	14041	tcgcccttcc	ttccctccct	tttcttcttg	gtgtc							
III											mRNA start	
	13681	cagcgggccc	ggggttcggc	ctcagtcagg	cgctcagctc	cgtttcgggtt	tcacttccgg					
	13741	tggagggccc	cctctgagcg	ggcggcgggc	cgacggcgag	cgcgggcggc	ggcggg GACG					
	13801	GAGGCGCCGC	TGCCAGG ggg	cgtgcggcag	cg ggcggcg	gcggcggcg	cggcggcggc					
	13861	ggagggcggcg	gcggcggcg	cggcggcggc	gg ctggg CCT	CGAGCGCCCG	CAGCCCAC ct					
	13921	ctcggggggcg	ggctcccggc	gctagcaggg	ctgaagagaa	gat ggaggag	ctggtggtgg					
											protein start	
	13981	aagtgcgggg	ctccaatggc	gctttctaca	aggtacttgg	ctctagggca	ggccccatct					
	14041	tcgcccttcc	ttccctccct	tttcttcttg	gtgtc							

Green capitalised:
FT Primers
(MIND Institute,
Tassone et al, JMD 2008)

383bp

Blue capitalised:
SFS Primers
(Asuragen,
Filipovic-Sadic et al,
Clin Chem 2010).

401bp

Purple capitalised:
FP2-RP2 Primers
(Abott,
Consensus paper,
JMD 2008).

224bp

Red letters: triplet region (sequence
obtained from GenBank with 20 repeats,
including the AGG).

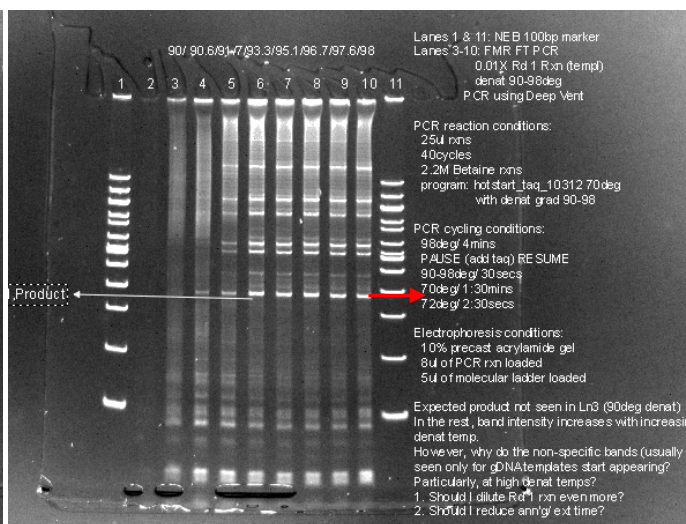
Detection methods: Sudha's work on FMR1

DV rxns in 0.5M NMP, 2.2M Betaine, and 1M TMSO at denaturation 98°C, annealing 70°C and extension 72°C.

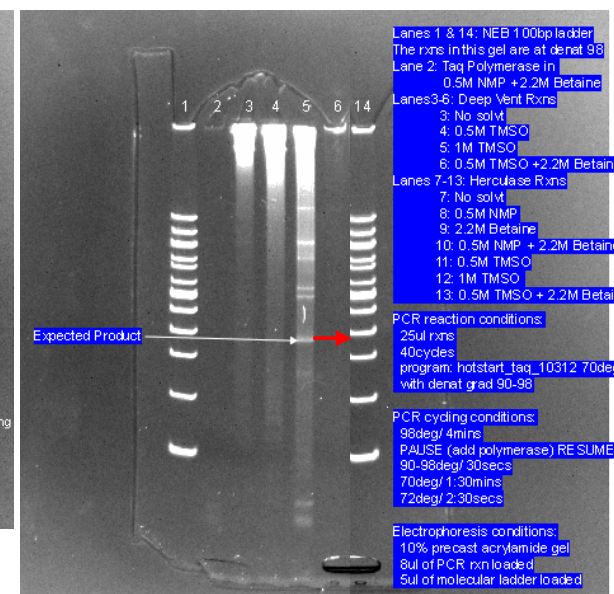
0.5M NMP



2.2M Betaine



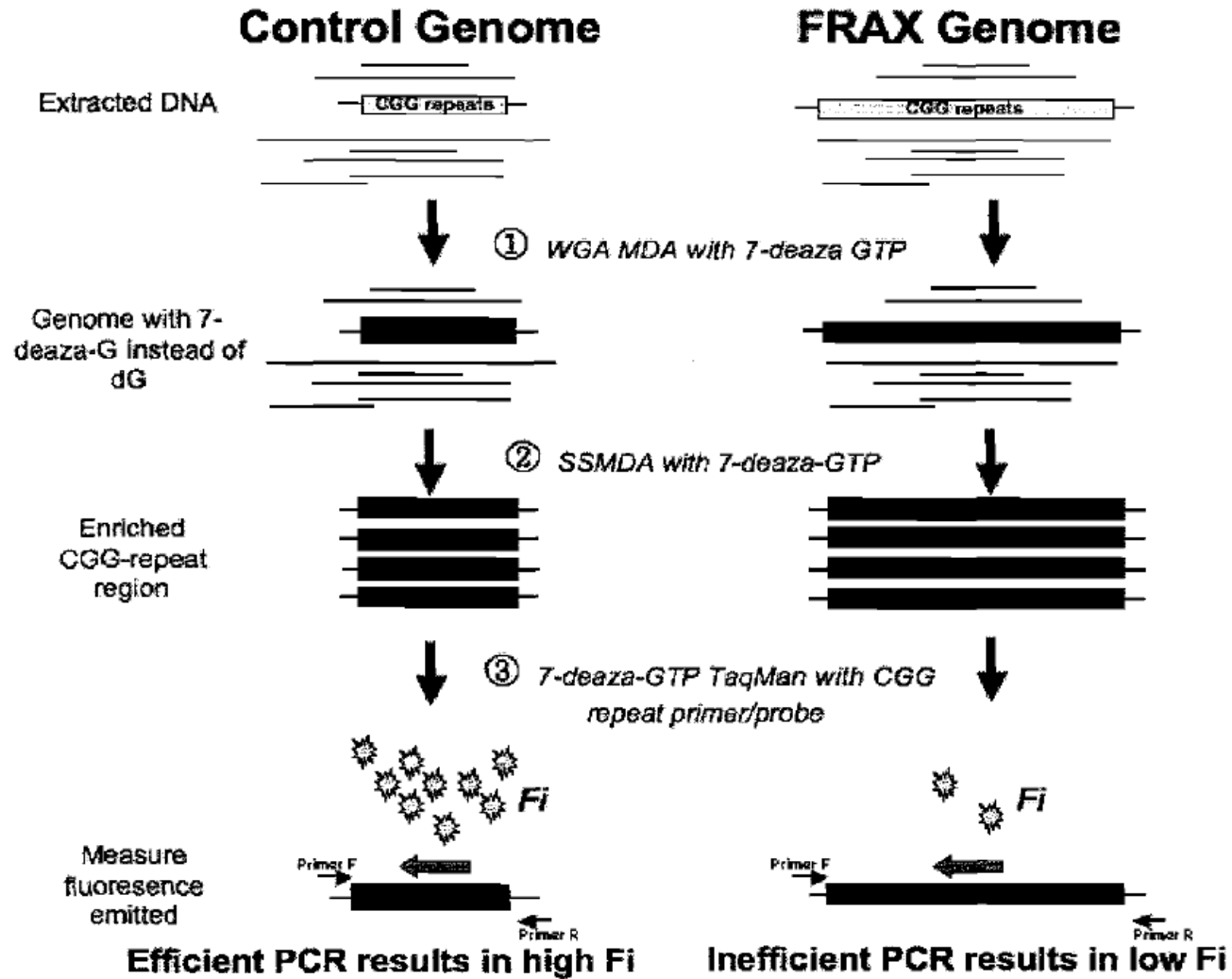
1M TMSO



Repeat-primed PCR vs. regular PCR

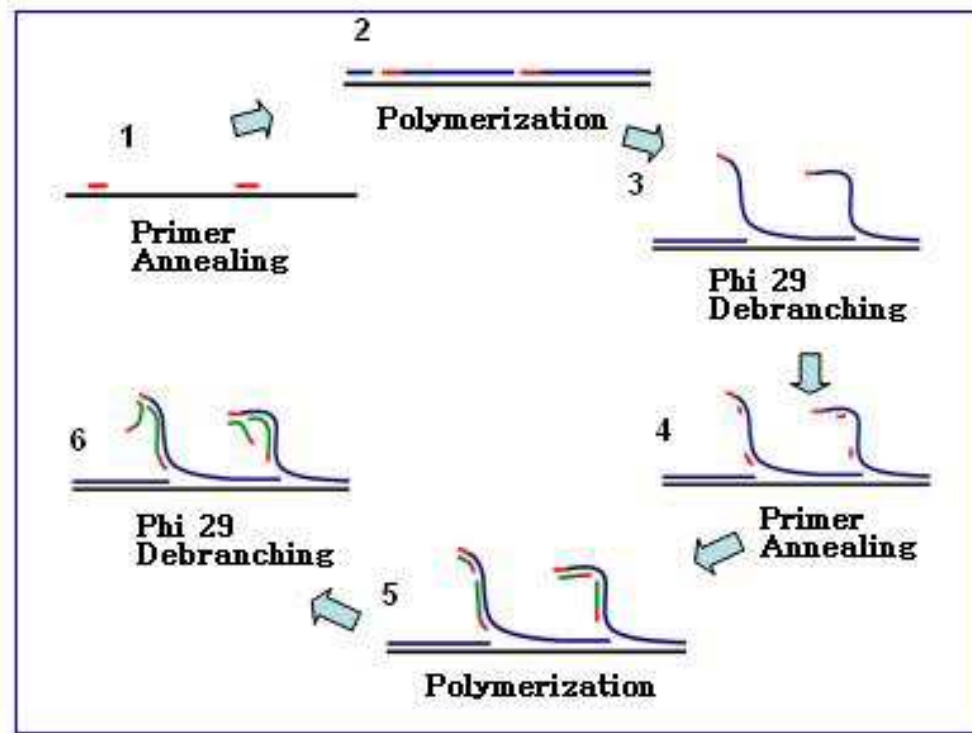
- Using regular PCR, the efficiency decreases as repeat number increases. For patient with large copy number (>100 repeats), regular PCR may not be able to give any signal.
- For patients with large copy number, repeat-primed PCR may not detect the exact number of repeats. But it can tell whether the copy number is larger than a threshold.
- Compared to PAGE, CE is more sensitive and easier to automate.

Detection methods: MDA-based

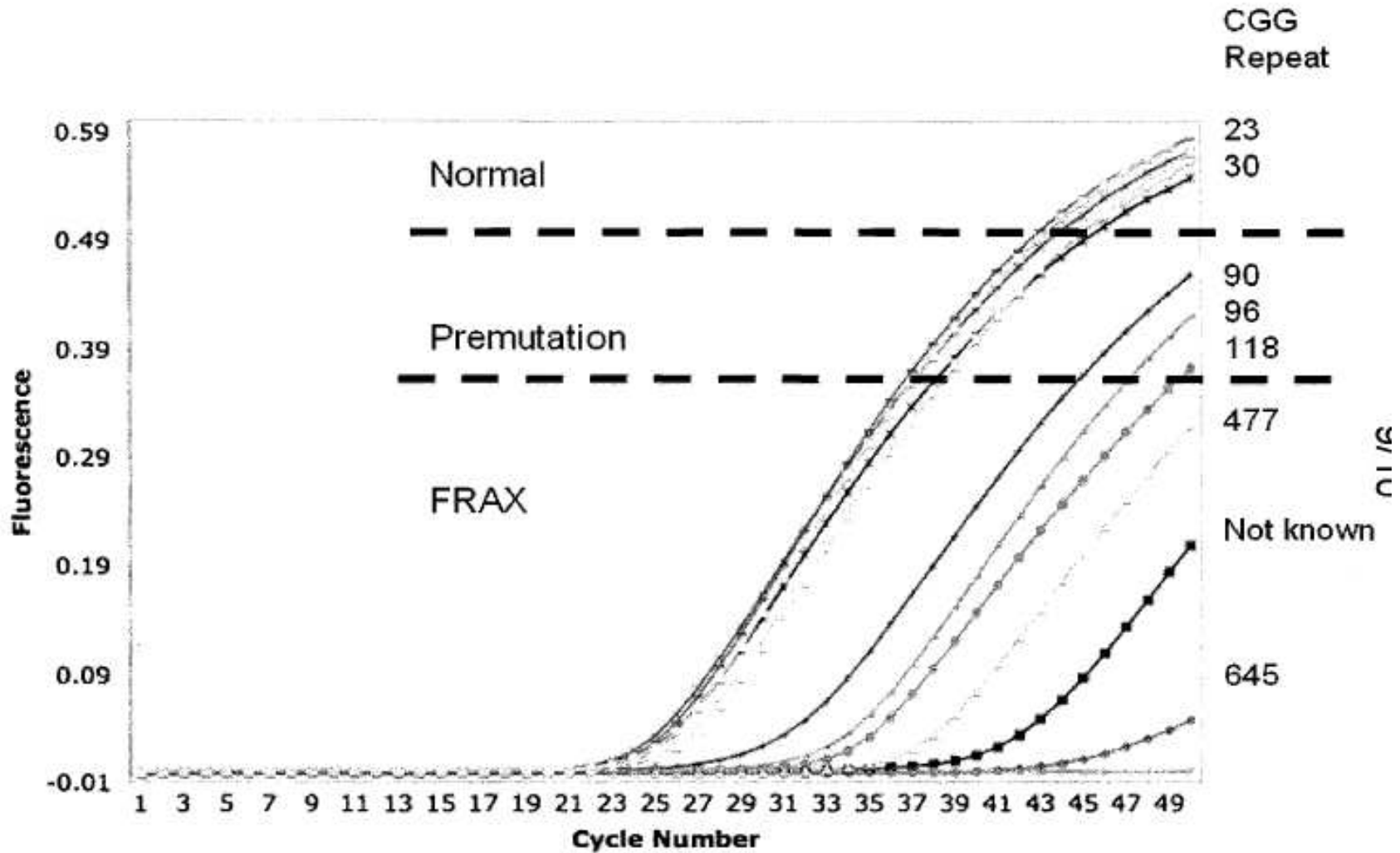


Multiple displacement amplification (MDA)

- DNA synthesis is carried out by a high processivity enzyme Φ 29 DNA polymerase, at a constant temperature.
- Compared to conventional PCR amplification techniques, MDA generates larger sized products with a lower error frequency.



Detection methods: MDA-based



What's next?

- ??